Determination of population and alignment of the ground state using two-photon nonresonant excitation

Andrew C. Kummel, Greg O. Sitz, and Richard N. Zare
Department of Chemistry, Stanford University, Stanford, California 94305

(Received 2 June 1986; accepted 3 September 1986)

A method is presented for determining the population $A_0^{(0)}$, the quadrupole alignment factors $A_0^{(2)}, A_1^{(2)}, A_2^{(2)}$, and the hexadecapole alignment factors $A_0^{(4)}, A_1^{(4)}, A_2^{(4)}, A_3^{(4)}, A_4^{(4)}$ for a (v,J) ground state distribution of a diatomic molecule probed by linearly polarized two-photon nonresonant excitation. General expressions are developed for the O, P, Q, R, and S branch transitions as a function of the rotational quantum number J. This treatment assumes that the resonant state reached by the two-photon transition is subsequently detected independent of its alignment. This can be achieved by $2 + n$ multiphoton ionization in which the ionization steps are saturated, or by $2 + 1$ laser induced fluorescence in which the fluorescence is collected independent of its polarization and spatial anisotropy. To extract the population and the eight alignment parameters the line intensities must be measured for several polarization settings of the laser beam. However, when the ground state distribution has cylindrical symmetry, only two alignment parameters are nonvanishing, $A_0^{(2)}$ and $A_0^{(4)}$, and they can be determined at a single polarization setting by comparing the line intensities of the different branches.

I. INTRODUCTION

This paper presents the theory required to extract both the scalar and vector properties of a ground state angular momentum distribution probed by two-photon absorption. The techniques presented allow the experimentalist to determine both the ground state population and eight higher order moments: $A_2^{(2)}, A_1^{(2)}, A_0^{(2)}, A_4^{(4)}, A_3^{(4)}, A_2^{(4)}, A_1^{(4)}, A_0^{(4)}$. In fact, it is impossible to extract the ground state rotational populations without also determining alignment factors because for two-photon excitation there are no magic angles which set all the higher order moments to zero even if the ground state angular momentum distribution has cylindrical symmetry.

A similar analysis has already been carried out for $1 + 1$ laser induced fluorescence (LIF). Case, McClelland, and Herschbach (CMH)[1] use a density matrix approach which is completely general. Greene and Zare (GZ)[2] use a spherical tensor formalism, taken from Fano and Macek (FM),[3] to treat the case where the ground state distribution has cylindrical symmetry. McCaffery and co-workers employ the density matrix formalism to investigate the $1 + 1$ LIF case in which the probe light is circularly or linearly polarized.[4] Jacobs and Zare[5] have investigated the combined effects of saturation and optical pumping for $1 + 1$ multiphoton ionization (MPI).

We treat a different case: two-photon absorption. This treatment can be applied to both $2 + 1$ LIF or to $2 + n$ MPI. We follow the example of GZ and avoid the use of the density matrix formalism since this would make the results appear quite complicated. Our treatment is basically a generalization of the GZ formalism to allow the ground state to be noncylindrically symmetric and to allow the one-photon state to be a virtual state.

Bray and Hochstrasser (BH),[6] as well as McClain and Harris,[7] and Halpern, Zacharias, and Wallenstein[8] developed formulas which allow the determination of the ground state rotational distribution if the spatial distribution of the ground state angular momentum is isotropic. Bain and McCaffery[4] have used the density matrix formalism to treat the case of two-photon absorption for a $\Delta J = \pm 2$ transition, but did not treat the case where the absorption can go via one of several virtual states as it may for $\Delta J = 0, \pm 1$ transitions. Chein and Yeung[9] as well as Dubs, Brühlmann, and Huber[10] have considered $2 + 1$ LIF. Both McClain[11] and Nascimento[12] have discussed the use of two-photon absorption in determining the symmetry of the excited/resonant state. Two-photon absorption spectroscopy has been used by Monson and McClain[13] as well as Michl and Thulstrup[14] to determine the polarization of the ground state for condensed phase systems.

The techniques developed in this paper are applicable to atoms, diatomic molecules, as well as linear and symmetric top polyatomic molecules which have unperturbed states that can be reached by two-photon excitation. Generalization to asymmetric top molecules is straightforward. Many diatomic molecules have already been detected using either $2 + 1$ MPI or $2 + 2$ MPI, for example: H_2,[15] N_2,[16] CO,[17] NO,[18], O_2,[19] and HCl.[20] In all likelihood this list will grow rapidly.

This paper is intended as a guide to the experimentalist. Toward this end, we present in Sec. II the formulas needed to convert raw spectroscopic data into populations and alignment factors, but we defer derivations until the Appendix. The basic results are summarized in Tables I–IV and are readily reduced to computer programs. In Sec. III we give an example of how to extract the population and alignment factors from recorded line intensities, and we discuss the meaning of the higher order alignment moments. In Sec. IV several special cases are presented which can be used to check the numerical evaluation of the formulas and to assist the design of experiments.

 0021-9606/86/246874-24$02.10 © 1986 American Institute of Physics

Downloaded 02 Jun 2011 to 171.66.83.218. Redistribution subject to AIP license or copyright; see http://jcp.aip.org/about/rights_and_permissions

II. MOMENT EXPANSION OF THE TWO-PHOTON TRANSITION PROBABILITY

The two-photon transition rate for a linear molecule can be found from the corresponding expression for single-photon resonance fluorescence by a simple generalization. The starting point is the expression for single-photon LIF [see Eq. (27) of GZ]:

$$I = C \sum_{M_f} \left\langle \left| \sum_{M_e} (J_f, M_f, \Lambda_f | \hat{\mathbf{e}}_d \cdot \mathbf{r}_1 | J_e, M_e, \Lambda_e) \times (J_e, M_e, \Lambda_e | \hat{\mathbf{e}}_a \cdot \mathbf{r}_2 | J_i, M_i, \Lambda_i) \right|^2 \right\rangle . \quad (1)$$

Here, C is a proportionality constant, and the brackets $\langle\ \rangle$ represent a weighted average over all initial states M_i. The resonance fluorescence process describes a one-photon electric dipole transition from the initial state i, characterized by the quantum numbers J_i, M_i, Λ_i, to the excited state e, characterized by J_e, M_e, Λ_e, followed by a one-photon dipole transition from the excited state to the final state f, characterized by J_f, M_f, Λ_f. Here $\hat{\mathbf{e}}_d$ and $\hat{\mathbf{e}}_a$ are the polarization vectors of the detected and absorbed photons. As is well known, all M_e must be summed over before squaring, i.e., the various $M_i \to M_e \to M_f$ paths are indistinguishable, and hence interfere. In sharp contrast to single-photon resonance fluorescence, a two-photon transition from i to f has its single-photon excited state replaced by a virtual state. In this virtual state the values of J_e and Λ_e are not unique, and when calculating the intensity we must sum over all possible paths, as shown in Fig. 1, including those with different J_e and Λ_e as well as those with different M_e. Consequently, Eq. (1) is altered to read

$$I = C \sum_{M_f} \left\langle \left| \sum_{\substack{J_e, M_e, \Lambda_e \\ \gamma_e}} \frac{(J_f, M_f, \Lambda_f | \hat{\mathbf{e}}_d \cdot \mathbf{r}_1 | \gamma_e, J_e, M_e, \Lambda_e)(\gamma_e, J_e, M_e, \Lambda_e | \hat{\mathbf{e}}_a \cdot \mathbf{r}_2 | J_i, M_i, \Lambda_i)}{E_{ei} - h\nu + i(\Gamma_e/2)} \right|^2 \right\rangle . \quad (2)$$

We note that $\hat{\mathbf{e}}_a$ and $\hat{\mathbf{e}}_d$ now represent the unit polarization vectors of the first and second photons absorbed. In LIF $\hat{\mathbf{e}}_a$ and $\hat{\mathbf{e}}_d$ were independent; in this treatment we assume that $\hat{\mathbf{e}}_a$ and $\hat{\mathbf{e}}_d$ are parallel, i.e., both photons have the same linear polarization. E_{ei} is the energy difference between the initial and virtual rovibronic states. Γ_e is the total homogeneous linewidth of the virtual state. The index γ_e identifies different electronic states which contribute to the virtual state. Using a similar treatment as carried out in GZ, we can recast Eq. (2) into a sum over tensor moments. Each term involves a product of a moment of the two-photon line strength, P_q^k, a moment of the ground state distribution, $A_q^{(k)}$, and the population in the state J_i, $n(J_i)$. As shown in the Appendix, Eq. (2) may be rewritten as

$$I = C(\det) \sum_{k,q} P_q^k(J_i, \Lambda_i, J_f, \Lambda_f; \Omega) A_q^{(k)}(J_i) n(J_i), \quad (3)$$

where

$$P_q^k(J_i, \Lambda_i, J_f, \Lambda_f; \Omega) = D(q) b^k(J_i) g^k(J_i) \sum_{k_d, k_a} (-1)^k \epsilon(k_d, k_a, k, q; \Omega_{\text{lab}}) \times \sum_{J_e, \Lambda_e, J'_e, \Lambda'_e} S(J_i, \Lambda_i, J_e, \Lambda_e, J'_e, \Lambda'_e, J_f, \Lambda_f) \times h(k_d, k_a, k, J_i, J_e, J'_e, J_f), \quad (4)$$

$k = 0,2,4$ and $q = 0,1,2,3,4$ are the rank and component of the ground state distribution; $k_d = 0,2$ and $k_a = 0,2$ are the ranks of the square of the first and second photons; and $J_e, \Lambda_e, J'_e, \Lambda'_e$ are subject to the usual dipole selection rules with respect to J_i, Λ_i and J_f, Λ_f.

Equations (3) and (4) represent the machinery needed

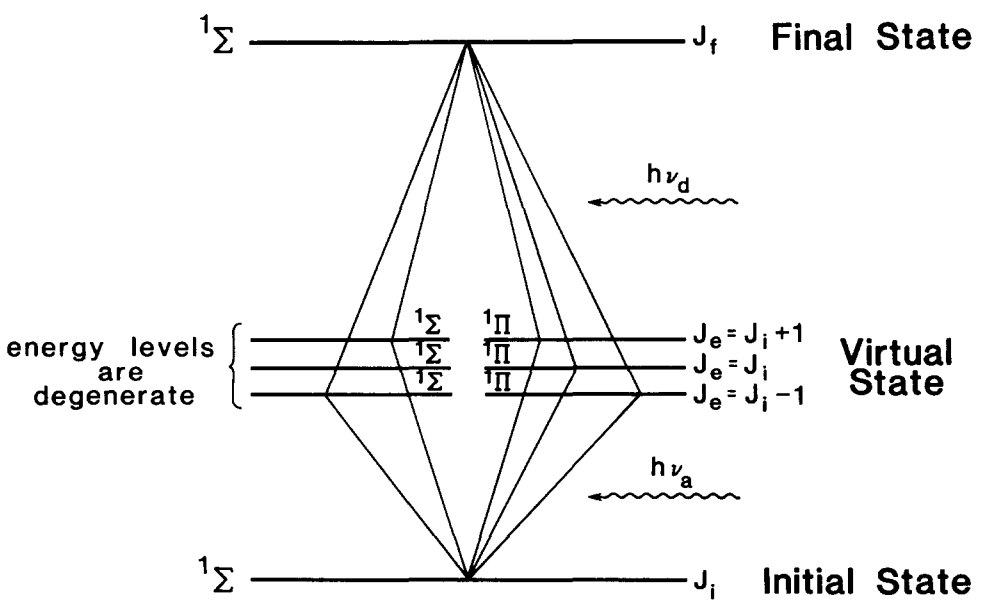

FIG. 1. Schematic diagram of a two-photon process through a virtual state and the consequent interference between indistinguishable paths.

Downloaded 02 Jun 2011 to 171.66.83.218. Redistribution subject to AIP license or copyright; see http://jcp.aip.org/about/rights_and_permissions

for reducing two-photon spectra to ground state population and alignment factors. In what follows we discuss each of the terms appearing in these two equations. The equations and nomenclature for these terms are summarized in Tables I and IV, and V. Equations (3) and (4) assume that the laser beam propagates along the y axis where the z axis is fixed in space and taken to be the axis of cylindrical symmetry, if such symmetry exists. All other cases are presented in Tables II and III.

A. The detection-sensitivity constant, C(det)

In general the experimentally determined intensities are in arbitrary units. The detection-sensitivity constant $C(\mathrm{det})$ converts the calculated intensities into the experimentally recorded ones. The magnitude of this constant depends on the amount of laser light, the sensitivity of the ion/photon detector, the magnitude of the radial part of the transition dipole moment integrals (see Sec. II H), etc. In general these factors are unknown. However, we assume that they are the same for all the recorded transitions. Hence, these detection and sensitivity factors can be grouped together into an overall constant, $C(\mathrm{det})$, which is independent of all the "initial," "excited," and "final" state rotational quantum numbers.

B. The population, $n(J_i)$

The population of the ground state, the total number of molecules of all polarizations in a given rotational state, J_i, is denoted by $n(J_i)$. This population incorporates the rotational degeneracy but not the degeneracy of nuclear or electronic spin because $g^k(J_i)$ and $g^k(N_i)$ incorporate these degeneracies. Hence for a Boltzmann distribution it equals

$$n(J_i) = (2J_i + 1)\exp[-E(J_i)/kT]. \tag{5}$$

We have omitted the division by the partition function in the expression for $n(J_i)$ since it can be absorbed into the overall detection-sensitivity constant, $C(\mathrm{det})$.

C. The moments of the ground state distribution, $A_q^{(k)}$

The ground state alignment of $\mathbf{J}_i$ is expanded into its spherical tensor components $A_q^{(k)}(J_i)$, where we follow the normalization conventions first introduced by FM and employed by GZ. Here we take the $A_q^{(k)}$ to be the real part of the expectation value of $J_q^{(k)}$, the spherical tensor components of the angular momentum operator.[21] Specifically:

$$A_q^{(k)}(J_i) = c(k)\mathrm{Re}\langle(J_iM_i\Lambda_i|J_q^{(k)}|J_iM_i\Lambda_i)\rangle/[(J_iM_i\Lambda_i|\mathbf{J}^2|J_iM_i\Lambda_i)]^{k/2}, \tag{6}$$

where

$$c(k=0) = 1, \tag{7a}$$

$$c(k=2) = (6)^{1/2}, \tag{7b}$$

$$c(k=4) = (35/8)^{1/2}. \tag{7c}$$

The normalization constants insure that we follow the GZ normalization. The results are listed in Table VI for $k = 0,2,4$ and $q = 0,1,2,3,4$. The $J_q^{(k)}$ are nothing more than spherical tensor operators made up from J_x, J_y, and J_z which satisfy the rotational transformation properties of a spherical tensor of rank k and component q and the commutation rules for angular momentum operators.

It is important to note that we have chosen a normalization in which $A_0^{(0)}(J_i)$ is always equal to one. Hence, the population is independent of the moments, and all the moments have finite limits. In Sec. III, we explicitly show how to extract both the population and the alignment factors from experimental line intensities. In that section we refer to the $A_q^{(k)}(J_i)$ as the reduced moments since this set of moments has the normalization $A_0^{(0)}(J_i) = 1$.

D. The moments of the line strength, $P_q^k(J_i,\Lambda_i,J_f,\Lambda_f;\Omega)$

The P_q^k represent the moments of the line strength for a system geometry described by Ω. We factor the intensity equation into spherical tensor moments, $A_q^{(k)}$, each of which is associated with its own line strength factor P_q^k.

TABLE I. The two-photon transition probability for coincident lab and detector frames where the laser propagation direction is along the y axis of the lab frame.

$$I = C(\mathrm{det})\sum_{k,q} P_q^k(J_i,\Lambda_i,J_f,\Lambda_f;\Omega)A_q^{(k)}(J_i)n(J_i),$$

$$P_q^k(J_i,\Lambda_i,J_f,\Lambda_f;\Omega) = D(q)b^k(J_i)g^k(J_i)\sum_{k_d,k_a}(-1)^k\epsilon(k_d,k_a,k,q;\Omega_{\mathrm{lab}})$$

$$\times\sum_{J_e,\Lambda_e,J_e',\Lambda_e'} S(J_i,\Lambda_i,J_e,\Lambda_e,J_e',\Lambda_e',J_f,\Lambda_f)h(k_d,k_a,k,J_i,J_e,J_e',J_f),$$

where $k = 0,2,4$; $q = 0,1,2,3,4$ but $q \leqslant k$; $k_d = 0,2$; $k_a = 0,2$.

$$A_q^{(k)}(J_i) = c(k)\mathrm{Re}\langle(J_iM_i\Lambda_i|J_q^{(k)}|J_iM_i\Lambda_i)\rangle/[(J_iM_i\Lambda_i|\mathbf{J}^2|J_iM_i\Lambda_i)]^{k/2},$$

$$\epsilon(k_a,k_d,k,q;\theta,0,\chi)(\mathrm{lab}) = [4\pi(2k_a+1)(2k_d+1)]^{1/2}$$

$$\times\begin{pmatrix}1 & 1 & k_d\\ 0 & 0 & 0\end{pmatrix}\begin{pmatrix}1 & 1 & k_a\\ 0 & 0 & 0\end{pmatrix}\begin{pmatrix}k_d & k_a & k\\ 0 & 0 & 0\end{pmatrix}Y_q^{(k)}(\theta,0).^{a}$$

[a] Note: the equation for ϵ is only valid for even k.

Downloaded 02 Jun 2011 to 171.66.83.218. Redistribution subject to AIP license or copyright; see http://jcp.aip.org/about/rights_and_permissions

TABLE II. The two-photon transition probability for noncoincident lab and detector frames where the laser propagation direction lies in the x–y plane of the lab frame of reference.

$$I = C(\text{det}) \sum_{k,q} [P_{q+}^{\{k\}}(J_i,\Lambda_i,J_f,\Lambda_f;\Omega)A_{q+}^{\{k\}}(J_i) + P_{q-}^{\{k\}}(J_i,\Lambda_i,J_f,\Lambda_f;\Omega)A_{q-}^{\{k\}}(J_i)]n(J_i),$$

$$P_{q\pm}^{\{k\}}(J_i,\Lambda_i,J_f,\Lambda_f;\Omega) = b^k(J_i)g^k(J_i) \sum_{k_d,k_a} [(-1)^k \epsilon_{q\pm}^{\{k\}}(k_d,k_a;\Omega_{\text{lab}})$$

$$\times \sum_{J_e\Lambda_e J_e'\Lambda_e'} S(J_i,\Lambda_i,J_e,\Lambda_e,J_e',\Lambda_e',J_f,\Lambda_f)h(k_d,k_a,k,J_i,J_e,J_e',J_f),$$

where $k = 0,2,4$; $q = 0,1,2,3,4$ but $q \leqslant k$; $k_d = 0,2$; $k_a = 0,2$.

$$A_{q\pm}^{\{k\}}(J_i) = c(k)\langle (J_iM_i\Lambda_i|J_{q\pm}^{\{k\}}|J_iM_i\Lambda_i)\rangle / [(J_iM_i\Lambda_i|\mathbf{J}^2|J_iM_i\Lambda_i)]^{k/2},$$

$$\epsilon_{q+}^{\{k\}}(k_a,k_d;\theta,0,\chi)(\text{lab}) = [8\pi(2k_a+1)(2k_d+1)]^{1/2}$$

$$\times \begin{pmatrix} 1 & 1 & k_d \\ 0 & 0 & 0 \end{pmatrix} \begin{pmatrix} 1 & 1 & k_a \\ 0 & 0 & 0 \end{pmatrix} \begin{pmatrix} k_d & k_a & k \\ 0 & 0 & 0 \end{pmatrix} Y_q^{(k)}(\theta,0)\cos(q\chi),^{a}$$

$$\epsilon_{q-}^{\{k\}}(k_a,k_d;\theta,0,\chi)(\text{lab}) = [8\pi(2k_a+1)(2k_d+1)]^{1/2}$$

$$\times \begin{pmatrix} 1 & 1 & k_d \\ 0 & 0 & 0 \end{pmatrix} \begin{pmatrix} 1 & 1 & k_a \\ 0 & 0 & 0 \end{pmatrix} \begin{pmatrix} k_d & k_a & k \\ 0 & 0 & 0 \end{pmatrix} Y_q^{(k)}(\theta,0)\sin(q\chi).^{a}$$

[a] Note: the equations for ϵ are only valid for even k.

E. The alignment degeneracy factor, $D(q)$

In general, we must sum over all values of k and q in Eq. (3) to incorporate the orientation and alignment of the ground state $\mathbf{J}_i$ distribution. As shown in the Appendix, the two-photon absorption intensity for linearly polarized light is insensitive to any ground state moment with odd k. In general, q can be either positive or negative. However, we assume that the laser beam is propagating along the y axis of the lab frame, so that for fixed k the line strength factor, P_q^k, for q positive is degenerate with that for q negative. Hence, we only need to sum over all positive values of q and multiply the degenerate moments by two to get the intensity of any transition. We denoted the alignment degeneracy factor by $D(q)$, where

$$D(q=0) = 1 \tag{8a}$$

and

$$D(q \neq 0) = 2. \tag{8b}$$

F. Reduced matrix elements of the spherical tensor angular momentum operators, $b^k(J_i)$

The $b^k(J_i)$ are proportional to the reduced matrix elements of the angular momentum spherical tensor operator in the ground state. These functions, taken from GZ, are tabulated in Table VII and can be considered simply as scaling factors for the alignment moments of the ground state distribution:

$$b^k(J_i) = c(k)^{-1}\{[(J_iM_i\Lambda_i|\mathbf{J}^2|J_iM_i\Lambda_i)]^{k/2}\}/(J_i\|J^{(k)}\|J_i), \tag{9}$$

where $c(k)$ are defined in Eqs. (7a), (7b), and (7c). The

TABLE III. The two-photon transition probability for noncoincident lab and detector frames where the detection geometry is general.

$$I = C(\text{det}) \sum_{k,q} [P_{q+}^{\{k\}}(J_i,\Lambda_i,J_f,\Lambda_f;\Omega)A_{q+}^{\{k\}}(J_i) + P_{q-}^{\{k\}}(J_i,\Lambda_i,J_f,\Lambda_f;\Omega)A_{q-}^{\{k\}}(J_i)]n(J_i),$$

$$P_{q\pm}^{\{k\}}(J_i,\Lambda_i,J_f,\Lambda_f;\Omega) = b^k(J_i)g^k(J_i) \sum_{k_d,k_a} [(-1)^{(k)} \epsilon_{q\pm}^{\{k\}}(k_d,k_a;\Omega_{\text{lab}})$$

$$\times \sum_{J_e\Lambda_e J_e'\Lambda_e'} S(J_i,\Lambda_i,J_e,\Lambda_e,J_e',\Lambda_e',J_f,\Lambda_f)h(k_d,k_a,k,J_i,J_e,J_e',J_f),$$

where $k = 0,2,4$; $q = 0,1,2,3,4$ but $q \leqslant k$; $k_d = 0,2$; $k_a = 0,2$.

$$A_{q\pm}^{\{k\}}(J_i) = c(k)\langle (J_iM_i\Lambda_i|J_{q\pm}^{\{k\}}|J_iM_i\Lambda_i)\rangle / [(J_iM_i\Lambda_i|\mathbf{J}^2|J_iM_i\Lambda_i)]^{k/2},$$

$$\epsilon_{q\pm}^{\{k\}} = (1/2)^{-1/2}(i)^{(\pm 1-1)/2}[(-1)^q\epsilon_{+q}^{(k)} \pm \epsilon_{-q}^{(k)}] \quad \text{for } 0 < q \leqslant k,$$

$$\epsilon_{0+}^{\{k\}} = \epsilon_{+0}^{(k)}; \quad \epsilon_{0-}^{\{k\}} = 0 \quad \text{for } q = 0,$$

$$\epsilon_q^{(k)}(k_d,k_a;\theta,0)(\text{lab}) = \sum_{q'} D_{q,q'}^{(k_d)*}(\phi_u,\theta_u,\chi_u)\epsilon_{q'}^{(k)}(k_d,k_a;\theta,0)(\text{det}).$$

Downloaded 02 Jun 2011 to 171.66.83.218. Redistribution subject to AIP license or copyright; see http://jcp.aip.org/about/rights_and_permissions

TABLE IV. Parameters in the two-photon transition probability appearing in Tables I–III.

$n(J_i)$ = population of level J_i

$D(q=0)=1$

$D(q\neq 0)=2$

$b^k(J_i)=c(k)^{-1}\{[(J_iM_i\Lambda_i|\mathbf{J}^2|J_iM_i\Lambda_i)]^{k/2}\}/(J_i\|J^{(k)}\|J_i)$

$c(k=0)=1;\ c(k=2)=(6)^{1/2};\ c(k=4)=(35/8)^{1/2}$

$$g^k(J_i)=\sum_I\sum_{F_i}(2F_i+1)^2\begin{Bmatrix}F_i & F_i & k\\ J_i & J_i & I\end{Bmatrix}^2$$

$$g^k(N_i)=\sum_{J_i}(2J_i+1)^2\begin{Bmatrix}J_i & J_i & k\\ N_i & N_i & S\end{Bmatrix}^2 g^k(J_i)$$

$$S(J_i,\Lambda_i,J_e,\Lambda_e,J_e',\Lambda_e',J_f,\Lambda_f)=(J_e'\Lambda_e'\|r^{(1)}\|J_i\Lambda_i)^*(J_e\Lambda_e\|r^{(1)}\|J_i\Lambda_i)\times(J_f\Lambda_f\|r^{(1)}\|J_e'\Lambda_e')^*(J_f\Lambda_f\|r^{(1)}\|J_e\Lambda_e)$$

$$(J_2\Lambda_2\|r^{(1)}\|J_1\Lambda_1)=(4\pi/3)^{1/2}R_{21}^{(\Lambda_2-\Lambda_1)}(2J_2+1)^{1/2}(2J_1+1)^{1/2}\times(-1)^{(J_2-\Lambda_2)}\begin{pmatrix}J_1 & J_2 & 1\\ \Lambda_1 & -\Lambda_2 & \Lambda_2-\Lambda_1\end{pmatrix}$$

$$(J_2\Lambda_2\|r^{(1)}\|J_1\Lambda_1)^*=(-1)^{(J_2-J_1)}(J_1\Lambda_1\|r^{(1)}\|J_2\Lambda_2)$$

$$h(k_d,k_a,k,J_i,J_e,J_e',J_f)=(-1)^{(J_f+J_e'-k_d+1)}[(2k_d+1)(2k_a+1)(2k+1)]^{1/2}\times\begin{Bmatrix}J_e' & J_e & k_d\\ 1 & 1 & J_f\end{Bmatrix}\begin{Bmatrix}J_e' & 1 & J_i\\ J_e & 1 & J_i\\ k_d & k_a & k\end{Bmatrix}$$

$$\epsilon_q^{(k)}(k_a,k_d,k,q;\theta,0)(\det)=[4\pi(2k_a+1)(2k_d+1)]^{1/2}\times\begin{pmatrix}1 & 1 & k_d\\ 0 & 0 & 0\end{pmatrix}\begin{pmatrix}1 & 1 & k_a\\ 0 & 0 & 0\end{pmatrix}\begin{pmatrix}k_d & k_a & k\\ 0 & 0 & 0\end{pmatrix}Y_q^{(k)}(\theta,0)$$

constants, $c(k)$, insure that the $b^k(J_i)$ follow the GZ normalization.

G. The hyperfine and fine structure depolarization, $g^k(J_i)$ and $g^k(N_i)$

The hyperfine depolarization term is denoted by $g^k(J_i)$. For molecules with nonzero nuclear spin, the direction of **J** is not fixed in space. Rather **J** is coupled to the nuclear spin **I** to form a resultant **F**, the total angular momentum. We assume that the nuclear spin is isotropically distributed. Initially, $\mathbf{J}_i$ may be aligned, but shortly afterwards it will be partially randomized because of coupling to **I**. When the hyperfine structure is unresolved, we must account for this loss of alignment by multiplying each tensor moment of the line strength by a depolarization factor $g^k(J_i)$ given by

$$g^k(J_i)=\sum_I\sum_{F_i}(2F_i+1)^2\begin{Bmatrix}F_i & F_i & k\\ J_i & J_i & I\end{Bmatrix}^2. \tag{10}$$

This expression for $g^k(J_i)$ differs from that of Greene and Zare[2,22] in that we sum over all nuclear spin states weighted by their degeneracies.

Here the summation over I includes only those nuclear spins which couple to J_i. While all nuclear spins couple to all J_i for heteronuclear diatomics, for homonuclear diatomics only even I couple to even/odd J_i and only odd I couple to odd/even J_i depending on the inversion symmetry of the electronic state. Hence in the high J_i limit, $g^k(J_i)$ equals the nuclear spin degeneracy; in extracting the population of J_i, we do not need to divide the unreduced zeroth moment by the nuclear degeneracy since it is already included in the equation for $g^k(J_i)$.

The coupling of nuclear spin to $\mathbf{J}_i$ is not the only possible source of depolarization. If the ground state is a multiplet state in which the spin is randomly polarized, we must also account for $\mathbf{J}_i$ being depolarized by electronic spin, $\mathbf{S}_i$. Conversely, when electronic spin is coupled to the internuclear axis [Hund's case (a) and (c)], then $\mathbf{J}_i$ is not depolarized by $\mathbf{S}_i$.

For the special case of a diatomic in a pure Hund's case (b) coupling scheme, we can modify the equation for $g^k(J_i)$ to include both hyperfine depolarization and unresolved fine structure depolarization.[23] For Hund's case (b), we employ the notation that **Λ**, the orbital angular momentum, is added to **R**, the angular momentum of nuclear rotation to form **N**, the total angular momentum apart from spin. Then **N** is added to **S**, the electronic spin angular momentum, to form **J**, the total angular momentum apart from nuclear spin. The quantities we wish to determine are no longer the moments of $\mathbf{J}_i$ but rather the moments of $\mathbf{N}_i$. Hence, we must replace J_i by N_i in all the formulas for the line strength and multiply this by a depolarization factor for each N_i; this factor will be denoted $g^k(N_i)$:

Downloaded 02 Jun 2011 to 171.66.83.218. Redistribution subject to AIP license or copyright; see http://jcp.aip.org/about/rights_and_permissions

TABLE V. Nomenclature for the two-photon transition strength formula.

J_i = Rotational quantum number of the "initial"/ground state apart from the nuclear spin

J_e = Rotational quantum number of the "excited"/virtual state apart from nuclear spin

J_f = Rotational quantum number of the "final"/resonant state apart from nuclear spin

Λ_i = Orbital angular momentum quantum number of the initial state

Λ_e = Orbital angular momentum quantum number of the excited/virtual state

Λ_f = Orbital angular momentum quantum number of the final state

k_a = The rank for the square of the first photon

k_d = The rank for the square of the second photon

k = The rank for the ground state distribution

q = The component for the ground state distribution

Ω = Angles describing the geometry of the laser beam with respect to the coordinate system for the moments of the ground state distribution

θ = Angle of the laser polarization vector with respect to the z axis of the detector frame

ϕ = Angle of the laser polarization vector with respect to the y axis of the detector frame

χ = The angle between the y axis of the detector frame and the y axis of the lab frame

F_i = Total angular momentum quantum number of the ground state including nuclear spin

I = Nuclear spin quantum number

S = Electronic spin quantum number

N_i = Total angular momentum quantum number apart from spin for Hund's case (b) molecules

$$g^k(N_i) = \sum_{J_i} (2J_i + 1)^2 \begin{Bmatrix} J_i & J_i & k \\ N_i & N_i & S \end{Bmatrix}^2 g^k(J_i). \qquad (11)$$

Equation (11) differs from that of Guest, O'Halloran, and Zare[23] in that we have summed over all fine structure levels of an electronic state with a given S value. Hence, Eq. (11) does not have a $2S+1$ factor in its denominator and $n(J_i)$ in Eq. (5) does not have a $2S+1$ factor in its numerator.

H. The system geometry, $\epsilon(k_a,k_d,k,q;\Omega_{\rm lab})$

In describing the system geometry we must employ two space-fixed frames of reference: the lab frame and the detector frame. Though we are free to choose any orthogonal set of axes as our lab reference frame (x,y,z), this is not a trivial choice because in general one is not free to choose the z axis of the lab frame. In many instances a system has an inherent axis of cylindrical or near cylindrical symmetry; in order to take advantage of this and reduce the number of ground state alignment moments to two, $A_0^{(2)}$, $A_0^{(4)}$, we must designate the axis of cylindrical symmetry to be the lab frame z axis.

Until now, we have only considered the case in which the lab and detector frames coincide; we briefly depart from this restriction in order to clarify how the detection geometry affects the amount of information that can be obtained using two-photon absorption. The detector frame (x_d,y_d,z_d) is always constructed so that the laser is propagating along its y_d axis. We designate θ as the angle between the polarization vector of the laser and the z_d axis (see Fig. 2) and ϕ as the angle measured from the x_d axis to the projection of the polarization vector in the x_d–y_d plane. Since the laser is propagating along the y_d axis, ϕ must be 0. If the experiment can be designed so that the laser propagation direction is perpendicular to the axis of symmetry, we are free to designate the laser propagation direction to also be the y axis of the lab frame. This is advantageous because when the laser is propagating along the lab frame y axis, the lab and detector frames coincide, as shown in Fig. 2.

In what follows, the z axis of the detector frame is assumed to be parallel to the z axis of the lab frame and the detector is assumed to lie in the x–y plane of the lab frame. Here, χ is designated as the angle between the y axis of the detector frame and the y axis of the lab frame (see Fig. 2); in the Appendix we allow the detector to be positioned anywhere in the lab frame.

The angle θ is the parameter which will be varied in order to determine the alignment moments. It is a convenient parameter because its variation can be accomplished without the apparatus being reconfigured. Unfortunately, if the detection geometry is fixed, the line strength factors for the noncylindrically symmetric moments, $A_4^{(4)}$, $A_2^{(4)}$, and $A_2^{(2)}$, are linearly dependent upon those for the cylindrically symmetric moments, $A_0^{(4)}$, $A_0^{(2)}$, and $A_0^{(0)}$, except at $\theta = 0°$.

The geometric factor ϵ for $\chi = 0$ has the explicit form:

$$\epsilon(k_a,k_d,k,q;\Omega_{\rm lab}) = [4\pi(2k_a+1)(2k_d+1)]^{1/2} \times \begin{pmatrix} 1 & 1 & k_d \\ 0 & 0 & 0 \end{pmatrix} \begin{pmatrix} 1 & 1 & k_a \\ 0 & 0 & 0 \end{pmatrix} \times \begin{pmatrix} k_d & k_a & k \\ 0 & 0 & 0 \end{pmatrix} Y_q^{(k)}(\theta,0), \qquad (12)$$

where the $Y_q^{(k)}(\theta,\phi) \equiv Y_{kq}(\theta,\phi)$ are the spherical harmonics. For the special case that $\phi = 0$,

$$Y_0^{(k)}(\theta,0) = [(2k+1)/4\pi]^{1/2} P_k(\cos\theta).$$

Explicit forms of the $Y_q^{(k)}(\theta,\phi)$ are listed in Mathews,[24] as well as in Pauling and Wilson.[25] The expression for ϵ for $\chi \neq 0$ are given in the Appendix and in Tables II and III.

I. Reduced matrix elements of the dipole moment operator, $S(J_i,\Lambda_i,J_e,\Lambda_e,J_e',\Lambda_e',J_f,\Lambda_f)$

The S terms in Eq. (4) are the reduced matrix elements of the dipole moment operators. The square of any one of these reduced matrix elements is equal to a Hönl–London factor. Hence we can think of this term as being the portion of the line strength which is independent of the coupling between the photons, the coupling between the angular momentum vectors, and the anisotropy of the ground state distribution. Explicitly,

Downloaded 02 Jun 2011 to 171.66.83.218. Redistribution subject to AIP license or copyright; see http://jcp.aip.org/about/rights_and_permissions

TABLE VI. Expressions for the moments of the ground state state distribution which can be extracted from a two-photon transition using linearly polarized excitation. The moments employ the GZ normalization and hence differ from those of CMH[a] by a constant which is a function of the rank k, but not the component q. Operators with multiple subscripts represent symmetric sums of all permutations. For example: $J_{xy} = J_xJ_y + J_yJ_x$. $\langle|\mathbf{J}^2|\rangle$ is the magnitude of the vector squared, i.e., $\langle|\mathbf{J}|\rangle = [J(J+1)]^{1/2}$.

The angular momentum spherical tensor operators expressed as functions of the raising and lowering operators[b]

$$J_0^{(0)} = 1$$

$$J_0^{(1)} = J_z$$

$$J_{\pm 1}^{(1)} = \mp (2)^{-1/2} J_\pm$$

$$J_0^{(2)} = (6)^{-1/2}(3J_z^2 - \mathbf{J}^2)$$

$$J_{\pm 1}^{(2)} = \mp J_\pm (2J_z \pm 1)$$

$$J_{\pm 2}^{(2)} = (1/2)(J_\pm)^2$$

$$J_0^{(3)} = [(10)^{-1/2}](5J_z^2 - 3\mathbf{J}^2 + 1)J_z$$

$$J_{\pm 1}^{(3)} = \mp [(30)^{1/2}/20] J_\pm (5J_z^2 - \mathbf{J}^2 \pm 5J_z + 2)$$

$$J_{\pm 2}^{(3)} = [(3)^{1/2}/2](J_\pm)^2(J_z \pm 1)$$

$$J_{\pm 3}^{(3)} = \mp [(2)^{-1/2}/2](J_\pm)^3$$

$$J_0^{(4)} = [(70)^{-1/2}/2](35J_z^4 - 30J_z^2\mathbf{J}^2 + 3\mathbf{J}^4 + 25J_z^2 - 6\mathbf{J}^2)$$

$$J_{\pm 1}^{(4)} = \mp [(14)^{-1/2}/2] J_\pm (14J_z^3 - 6\mathbf{J}^2 J_z \pm 21J_z^2 \mp 3\mathbf{J}^2 + 19J_z \pm 6)$$

$$J_{\pm 2}^{(4)} = [(7)^{-1/2}/2](J_\pm)^2(7J_z^2 - \mathbf{J}^2 \pm 14J_z + 9)$$

$$J_{\pm 3}^{(4)} = \mp [(2)^{-1/2}/2](J_\pm)^3(2J_z \pm 3)$$

$$J_{\pm 4}^{(4)} = (1/4)(J_\pm)^4$$

where

$$J_\pm = J_x \pm iJ_y$$

$$(J_\pm)^2 = J_x^2 - J_y^2 \pm i(J_xJ_y + J_yJ_x)$$
$$= J_{x^2} - J_{y^2} \pm i(J_{xy})$$

$$(J_\pm)^3 = J_x^3 - (J_xJ_y^2 + J_yJ_xJ_y + J_y^2J_x) \pm i[(J_yJ_x^2 + J_xJ_yJ_x + J_x^2J_y) - J_y^3]$$
$$= J_{x^3} - J_{xy^2} \pm i(J_{yx^2} - J_{y^3})$$

$$(J_\pm)^4 = J_x^4 + J_y^4 - (J_x^2J_y^2 + J_yJ_x^2J_y + J_y^2J_x^2 + J_xJ_yJ_xJ_y + J_xJ_y^2J_x)$$
$$\pm i[(J_yJ_x^3 + J_xJ_yJ_x^2 + J_x^2J_yJ_x + J_x^3J_y) + (J_xJ_y^3 + J_yJ_xJ_y^2 + J_y^2J_xJ_y + J_x^3J_y)]$$
$$= J_{x^4} + J_{y^4} - J_{y^2x^2} \pm i(J_{yx^3} + J_{xy^3})$$

The moments of the ground state distribution as defined in Eq. (A61)

$$A_0^{(0)} = 1$$

$$A_0^{(2)}) = \langle(J_i|(3J_z^2 - \mathbf{J}^2)/\mathbf{J}^2|J_i)\rangle$$

$$A_1^{(2)} = -(6)^{1/2}\langle(J_i|J_x(2J_z+1)/(\mathbf{J}^2)|J_i)\rangle$$

$$A_2^{(2)} = (6)^{1/2}\langle(J_i|(J_{x^2} - J_{y^2})/(2\mathbf{J}^2)|J_i)\rangle$$

$$A_0^{(4)} = \langle(J_i|(35J_z^4 - 30J_z^2\mathbf{J}^2 + 3\mathbf{J}^4 + 25J_z^2 - 6\mathbf{J}^2)/(8\mathbf{J}^4)|J_i)\rangle$$

$$A_1^{(4)} = -(5)^{1/2}\langle(J_i|J_x(14J_z^3 - 6\mathbf{J}^2J_z + 21J_z^2 - 3\mathbf{J}^2 + 19J_z + 6)/(8\mathbf{J}^4)|J_i)\rangle$$

$$A_2^{(4)} = (5/2)^{1/2}\langle(J_i|(J_{x^2} - J_{y^2})(7J_z^2 - \mathbf{J}^2 + 14J_z + 9)/(4\mathbf{J}^4)|J_i)\rangle$$

$$A_3^{(4)} = -(35)^{1/2}\langle(J_i|(J_{x^3} - J_{xy^2})(2J_z+3)/(8\mathbf{J}^4)|J_i)\rangle$$

$$A_4^{(4)} = (35/2)^{1/2}\langle(J_i|(J_{x^4} + J_{y^4} - J_{x^2y^2})/(8\mathbf{J}^4)|J_i)\rangle$$

The "real tensor" moments of the ground state distribution as defined in Eq. (A52)

$$A_{0+}^{\{0\}} = 1$$

$$A_{0+}^{\{2\}} = \langle(J_i|(3J_z^2 - \mathbf{J}^2)/\mathbf{J}^2|J_i)\rangle$$

$$A_{1+}^{\{2\}} = -2(3)^{1/2}\langle(J_i|J_x(2J_z+1)/(\mathbf{J}^2)|J_i)\rangle$$

$$A_{1-}^{\{2\}} = 2(3)^{1/3}\langle(J_i|J_y(2J_z-1)/(\mathbf{J}^2)|J_i)\rangle$$

$$A_{2+}^{\{2\}} = (3)^{1/2}\langle(J_i|(J_{x^2} - J_{y^2})/(\mathbf{J}^2)|J_i)\rangle$$

$$A_{2-}^{\{2\}} = (3)^{1/2}\langle(J_i|(J_{xy})/(\mathbf{J}^2)|J_i)\rangle$$

$$A_{0+}^{\{4\}} = \langle(J_i|(35J_z^4 - 30J_z^2\mathbf{J}^2 + 3\mathbf{J}^4 + 25J_z^2 - 6\mathbf{J}^2)/(8\mathbf{J}^4)|J_i)\rangle$$

Downloaded 02 Jun 2011 to 171.66.83.218. Redistribution subject to AIP license or copyright; see http://jcp.aip.org/about/rights_and_permissions

TABLE VI (*continued*).

$$A_{1+}^{\{4\}} = -(10)^{1/2}\langle(J_i|J_x(14J_z^3 - 6\mathbf{J}^2J_z + 21J_z^2 - 3\mathbf{J}^2 + 19J_z + 6)/(8\mathbf{J}^4)|J_i)\rangle$$
$$A_{1-}^{\{4\}} = (10)^{1/2}\langle(J_i|J_y(14J_z^3 - 6\mathbf{J}^2J_z - 21J_z^2 + 3\mathbf{J}^2 + 19J_z - 6)/(8\mathbf{J}^4)|J_i)\rangle$$
$$A_{2+}^{\{4\}} = (5)^{1/2}\langle(J_i|(J_{x^2} - J_{y^2})(7J_z^2 - \mathbf{J}^2 + 14J_z + 9)/(4\mathbf{J}^4)|J_i)\rangle$$
$$A_{2-}^{\{4\}} = (5)^{1/2}\langle(J_i|(J_{xy})(7J_z^2 - \mathbf{J}^2 - 14J_z + 9)/(4\mathbf{J}^4)|J_i)\rangle$$
$$A_{3+}^{\{4\}} = -(70)^{1/2}\langle(J_i|(J_{x^3} - J_{xy^2})(2J_z + 3)/(8\mathbf{J}^4)|J_i)\rangle$$
$$A_{3-}^{\{4\}} = (70)^{1/2}\langle(J_i|(J_{yx^2} - J_{y^3})(2J_z - 3)/(8\mathbf{J}^4)|J_i)\rangle$$
$$A_{4+}^{\{4\}} = (35)^{1/2}\langle(J_i|(J_{x^4} + J_{y^4} - J_{x^2y^2})/(8\mathbf{J}^4)|J_i)\rangle$$
$$A_{4-}^{\{4\}} = (35)^{1/2}\langle(J_i|(J_{yx^3} + J_{xy^3})/(8\mathbf{J}^4)|J_i)\rangle$$

[a] In Table I of CMH there appears to be some typographical errors in $J_{\pm 2}^{(4)}$, $J_0^{(4)}$, and $J_{\pm 1}^{(2)}$.
[b] The $J_q^{(k)}$ are generated from the $J_{\pm k}^{(k)} = [J_{\pm 1}^{(1)}]^k$ by applying the raising and lowering operators $J_\pm = J_x \pm iJ_y = \mp(2)^{1/2}J_{\pm 1}^{(1)}$ and using the relationship $[J_\pm, J_q^{(k)}] = [k(k+1) - q(q\pm 1)]^{1/2}J_{q\pm 1}^{(k)}$.

$$S(J_i,\Lambda_i,J_e,\Lambda_e,J'_e,\Lambda'_e,J_f,\Lambda_f) = (J'_e\Lambda'_e\|r^{(1)}\|J_i\Lambda_i)^*(J_e\Lambda_e\|r^{(1)}\|J_i\Lambda_i) \times (J_f\Lambda_f\|r^{(1)}\|J'_e\Lambda'_e)^*(J_f\Lambda_f\|r^{(1)}\|J_e\Lambda_e), \quad (13)$$

where

$$(J_2\Lambda_2\|r^{(1)}\|J_1\Lambda_1) = (4\pi/3)^{1/2}R_{21}^{(\Lambda_2-\Lambda_1)}(2J_2+1)^{1/2}(2J_1+1)^{1/2} \times (-1)^{(J_2-\Lambda_2)}\begin{pmatrix} J_1 & J_2 & 1 \\ \Lambda_1 & -\Lambda_2 & \Lambda_2-\Lambda_1 \end{pmatrix} \quad (14)$$

and

$$(J_2\Lambda_2\|r^{(1)}\|J_1\Lambda_1)^* = (-1)^{(J_2-J_1)}(J_1\Lambda_1\|r^{(1)}\|J_2\Lambda_2) \quad (15)$$

and $R_{21}^{(\Lambda_2-\Lambda_1)}$ equals the radial part of the transition dipole moment integral between the states, Λ_2,Λ_1, in the Born–Oppenheimer approximation weighted by a detuning parameter.

In general the radial integrals are unknown, but they are usually included in the detection-sensitivity constant, $C(\text{det})$. In some cases, such as a Σ–Σ transition, we must know the ratio of the products of the radial integrals for excitation via $\Sigma\to\Sigma\to\Sigma$ or via $\Sigma\to\Pi\to\Sigma$ pathways. In this case we can employ the technique suggested by Bray and Hochstrasser[6] of measuring the ratio of these radial integrals on an isotropic sample by comparing line intensities using linearly and circularly polarized light. We then use this path ratio as the radial integral terms in the above equation.

J. The angular momentum coupling terms, $h(k_d,k_a,k,J_i,J_e,J'_e,J_f)$

The $h(k_d,k_a,k,J_i,J_e,J'_e,J_f)$ in Eq. (4) represent the angular momentum coupling terms. They show how the moments of the square of the photon electric field vectors and the moments of the ground state alignment distribution are coupled to the angular momentum vectors of all three states. Explicitly,

$$h(k_d,k_a,k,J_i,J_e,J'_e,J_f) = (-1)^{(J_f+J'_e-k_d+1)} \times [(2k_d+1)(2k_a+1)(2k+1)]^{1/2} \times \begin{Bmatrix} J'_e & J_e & k_d \\ 1 & 1 & J_f \end{Bmatrix}\begin{Bmatrix} J'_e & 1 & J_i \\ J_e & 1 & J_i \\ k_d & k_a & k \end{Bmatrix}. \quad (16)$$

At first sight, Eq. (16) has a formidable appearance to the uninitiated because of the presence of the 6-*j* and 9-*j* symbols. These are fractions whose values can be found as the sums of products of 3-*j* symbols.[26–30] Hence, their presence should not deter the use of Eq. (16) because their values are readily calculated using numerical techniques.

III. AN EXAMPLE

In this section we calculate the moments of the line strength for a specific case and show how to convert line intensity measurements into the alignment moments of a ground state distribution. The molecular constants used are those for the two-photon transition, $N_2\ a\ ^1\Pi_g$–$X\ ^1\Sigma_g^+$.

A. The moments of the line strength as a function of J_i and θ

In Figs. 3 and 4 we have plotted the normalized moments of the line strength (including hyperfine depolarization) as a function of the angle of the laser polarization in the high J_i limit. The strength of the zeroth moment is independent of the polarization of the laser since it only reflects the population in the ground state and contains no spatial information. It is important to note that all the even q moments are symmetric about 90°. Consequently, when collecting data on a cylindrical symmetric distribution, the angle of polarization need not be varied outside 0° and 90°.

Inspection of the graphs for the noncylindrically symmetric moments shows that they all are strictly zero at

Downloaded 02 Jun 2011 to 171.66.83.218. Redistribution subject to AIP license or copyright; see http://jcp.aip.org/about/rights_and_permissions

TABLE VII. Expressions for the rescaling factors, $b^k(J_i)$. These expressions employ the GZ normalization.

$$b^0(J_i) = (2J_i+1)^{-1/2}$$

$$b^2(J_i) = \{J_i(J_i+1)/[(2J_i+3)(2J_i+1)(2J_i-1)]\}^{1/2}$$

$$b^4(J_i) = \frac{4J_i^2(J_i+1)^2}{[(J_i+2)(J_i+1)J_i(J_i-1)(2J_i+5)(2J_i+3)(2J_i+1)(2J_i-1)(2J_i-3)]^{1/2}}$$

$\theta = 0°$. This fact is quite advantageous because if we record the line intensities for three rotational branches at 0° then we can determine the three cylindrically symmetric moments of the ground state, whether or not the system has cylindrical symmetry.

Except for P_0^0 and a few rotational branches of P_4^4 and P_2^2, the line strength moments are rapidly changing functions of the laser polarization angle. This is quite unfortunate because in order to accurately measure the corresponding $A_q^{(k)}$, we need to record the line intensities at a large number of closely spaced polarization angles. In addition, the smoothly varying moments require us to record the data over the full range of polarization angles. Failure to do this will result in being unable to differentiate between contributions for pairs of $A_q^{(k)}$ which have similar $A_q^{(k)}$, for example P_4^4 and P_2^2.

In Fig. 5 we have plotted the line strength moments as a function of the rotational quantum number J_i. This figure has been constructed for $\theta = 15°$ and $q = 0$ because other values of θ and q would not change the shape of the plots but only the scales. Hence a plot of P_q^k vs J_i has the same appearance as a plot of P_0^k vs J_i for a given value of θ, and a change in θ causes just another rescaling. As Eqs. (4) and (12) show, P_q^k depends on θ and q only through the spherical harmonic term $Y_q^{(k)}(\theta,0)$, and this term does not affect the dependence of P_q^k on J_i.

In these figures we have omitted the moments of the line strengths, P_q^k, which are undefined or strictly zero. For the zeroth moment the lines $O(2), O(1), P(1), O(0), P(0)$, and $Q(0)$ do not exist because they connect ground state rotational levels to rotational levels less than one in a $^1\Pi$ state. $R(0)$ is strictly zero for a two-photon transition between a $^1\Sigma$ state and a $^1\Pi$ state. For the second moment we omit all the moments for those transitions which are undefined or strictly zero, and we omit all transitions with J_i less than one. J_i must be greater than or equal to one to exhibit a quadrupole moment. For the plot of the hexadecapole moment, we omit all transitions for J_i less than two since these cannot exhibit a hexadecapole moment.

Finally, in Fig. 6 we plot the hyperfine depolarization divided by the nuclear spin degeneracy vs the rotational quantum number J_i. This quantity is independent of both q and θ. All our calculations for P_q^k have included the hyper-

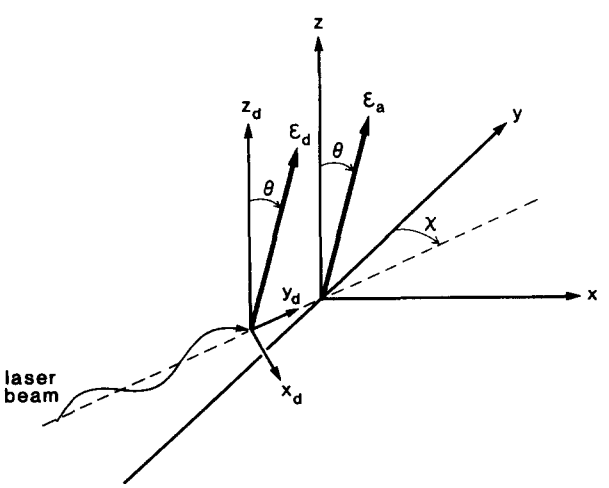

FIG. 2. The system geometry. The axes of the space-fixed frame are labeled x, y, and z while x_d, y_d, and z_d denote the axes of the detector fixed frame. Note that the laser beam propagates along the y_d axis making an angle χ with respect to the y axis of the space-fixed frame. The electric field vector is in the x_d–z_d plane at an angle θ with respect to z_d.

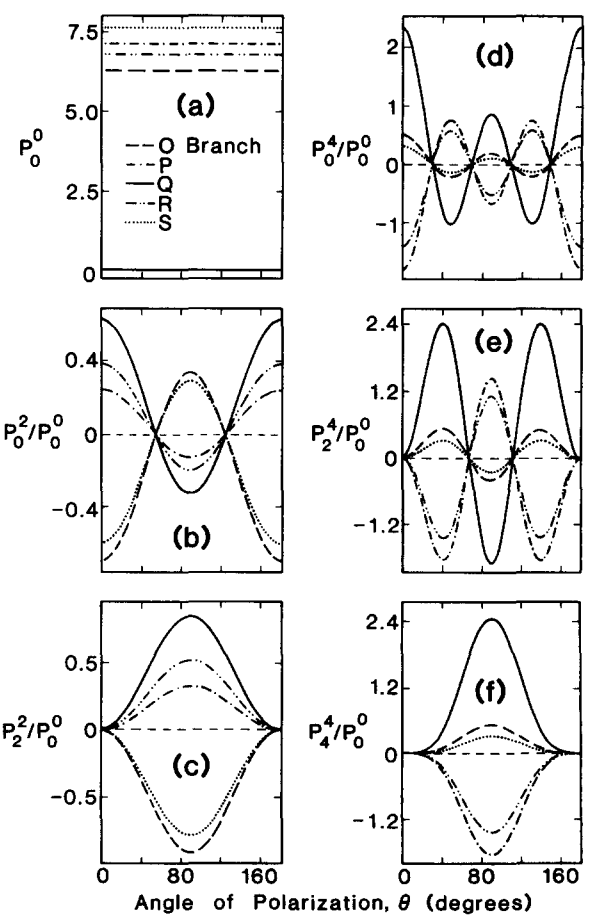

FIG. 3. The moments of the line strength factor with even components P_q^k vs the angle of polarization θ for the five rotational branches of $J_i = 20$ in the N_2 $a\,^1\Pi_g$–$X\,^1\Sigma_g^+$ two-photon transition. All P_q^k, except P_0^0, have been normalized with respect to P_0^0.

Downloaded 02 Jun 2011 to 171.66.83.218. Redistribution subject to AIP license or copyright; see http://jcp.aip.org/about/rights_and_permissions

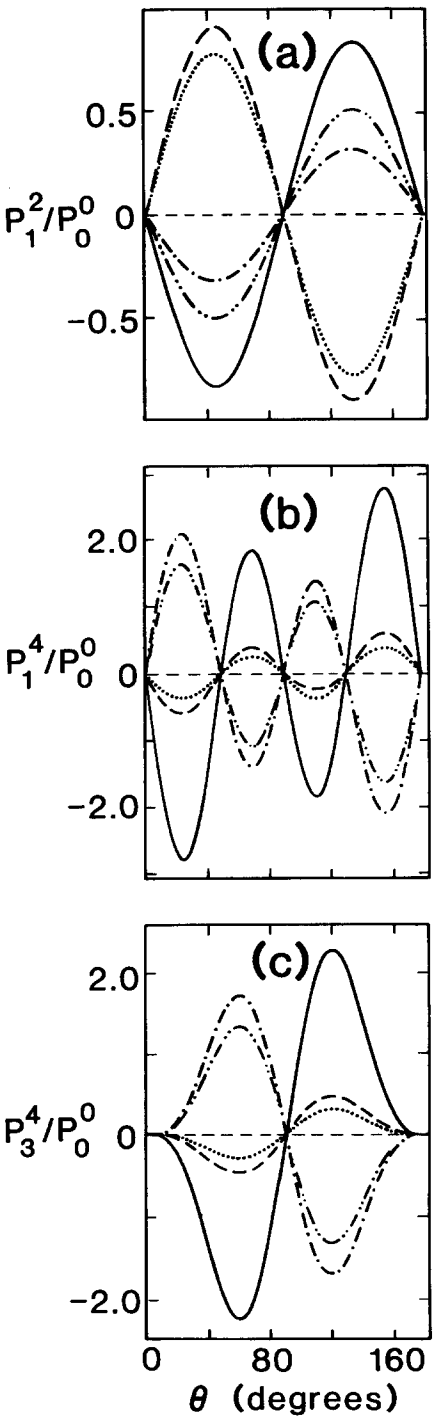

FIG. 4. The moments of the line strength factor with odd components P_q^k, vs the angle of polarization θ for the five rotational branches of $J_i = 20$ in the N_2 $a\ ^1\Pi_g$–$X\ ^1\Sigma_g^+$ two-photon transition. All P_q^k, except P_0^0, have been normalized with respect to P_0^0.

fine depolarization. For N_2, the even J_i couple with total nuclear spin 0 and 2. This implies that even at low J_i, the minimum value of the hyperfine depolarization is one sixth for even J_i. As J_i increases above the value of k, the hyperfine depolarization due to $I = 2$ decreases. The odd J_i only couple to the $I = 1$ and hence can become completely depolarized as J_i approaches zero. Though the graph of the hyperfine depolarization, $g^k(J_i)$ vs J_i, appears jagged, if we decompose it into separate plots for the even J_i, it becomes a smooth function.

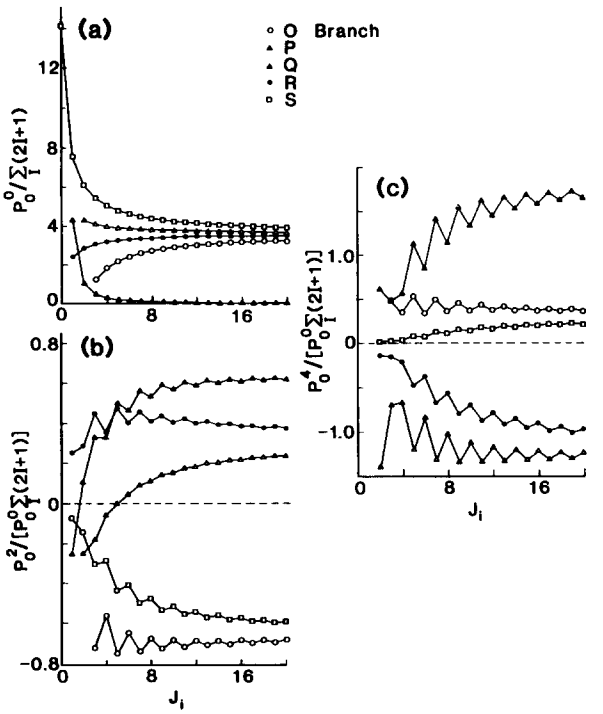

FIG. 5. The moments of the line strength factor P_q^k vs the ground state rotational quantum number for the five rotational branches at $\theta = 15°$ in the N_2 $a\ ^1\Pi_g$–$X\ ^1\Sigma_g^+$ two-photon transition. The moments of the P_q^k have been normalized with respect to the total nuclear hyperfine degeneracy of each J_i, and the higher order moments have been normalized with respect to the zeroth moment.

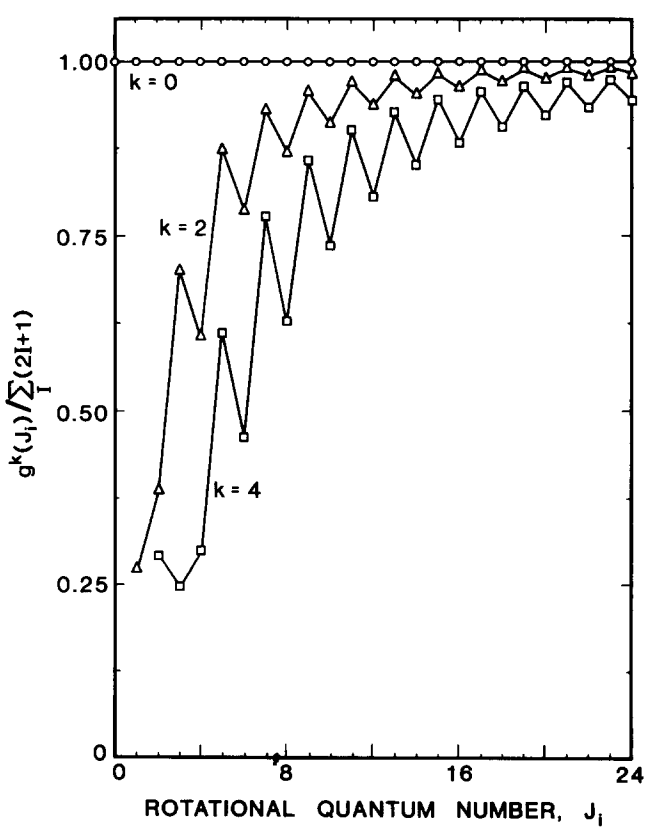

FIG. 6. The hyperfine depolarization factor for N_2 $X\ ^1\Sigma_g^+$ vs the ground state rotational quantum number for rank 0, 2, and 4 moments. The degeneracy factors have been normalized with respect to the total nuclear hyperfine degeneracy of each J_i.

Downloaded 02 Jun 2011 to 171.66.83.218. Redistribution subject to AIP license or copyright; see http://jcp.aip.org/about/rights_and_permissions

In the high J_i limit, $g^k(J_i)$ converges to the value for the nuclear spin degeneracy so we expect all the curves in Fig. 6 will converge toward unity in the high J_i limit. We anticipate that the curve for $k=4$ will converge the slowest since the hexadecapole moments are the most sensitive to depolarization.

B. Polar plots of the pure moments of a distribution

Before describing how to extract the moments of the ground state distribution, it seems only natural that we clearly depict the shapes of these moments so that we can visualize what it is that we are trying to determine. Let ground state distribution be denoted by $P(J,M)$ where the sum of $P(J,M)$ over all M is just the population, $n(J)$, of the level J. Then the moments of the ground state angular momentum distribution can be expressed as

$$A_q^{(k)}(J) = c(k)(JM|\mathbf{J}^2|JM)^{-k/2}\,\mathrm{Re}\sum_M P(J,M) \times (JM|J_q^{(k)}|JM)\Big/\sum_M P(J,M). \quad (17)$$

We solve Eq. (17) for $P(J,M)$ by multiplying both sides by $\mathrm{Re}\,\Sigma_{k,q}\,(2k+1)(JM'|J_q^{(k)}|JM')/(J\|J^{(k)}\|J)^2$:

$$n(J)\mathrm{Re}\sum_{k,q} A_q^{(k)}(2k+1)(JM|\mathbf{J}^2|JM)^{k/2} \times (JM'|J_q^{(k)}|JM')/[c(k)(J\|J^{(k)}\|J)^2] = \sum_M P(J,M)\mathrm{Re}\sum_{k,q}(2k+1)(J\|J^{(k)}\|J)^{-2} \times (JM'|J_q^{(k)}|JM')(JM|J_q^{(k)}|JM). \quad (18)$$

Application of the Wigner–Eckart theorem [see (Eq. (5.4.1) of Edmonds[29]] to both matrix elements on the right-hand side of Eq. (18) and the orthonormality of the resulting 3-j symbols [see (Eq. 3.7.7) of Edmonds[29]] gives

$$P(J,M) = n(J)\sum_{k,q}\xi(J,k)A_q^{(k)}(J)\mathrm{Re}[(JM|J_q^{(k)}|JM)], \quad (19)$$

where

$$\xi(J,k) = (2k+1)[J(J+1)]^{k/2}/[c(k)(J\|J^{(k)}\|J)^2] = (2k+1)c(k)[b^k(J)]^2/[J(J+1)]^{k/2} \quad (20)$$

and in Eq. (19) k ranges from 0 to $2J$ in integral steps and q ranges from $-k$ to k. Here $J_q^{(k)}$ is the angular momentum spherical tensor operator, and it has complex matrix elements. Again, $c(k)$ are the normalization constants defined in Eqs. (7a)–(7c) which insure that the $A_q^{(k)}$ follow the GZ normalization. Equation (19) represents the expansion of the ground state angular momentum distribution in the orientation and alignment factors $A_q^{(k)}$.

In the high J limit the expectation values of the angular momentum spherical tensor operators become equal to spherical harmonics multiplied by a conversion factor, $v(k) = [\mathrm{Re}(J_q^{(k)})/(\mathbf{J}^2)^{k/2}]/\{\mathrm{Re}[Y_q^{(k)}(\theta,\phi)]\}$; $v(0) = (4\pi)^{1/2}$, $v(2) = (8\pi/15)^{1/2}$, $v(4) = 4(2\pi/315)^{1/2}$. Thus for high J:

$$P(J,J_x,J_y,J_z) = n(J)\sum_{k,q}(2k+1)[b^k(J)]^2c(k) \times v(k)A_q^{(k)}(J)\mathrm{Re}[Y_q^{(k)}(\theta,\phi)], \quad (21)$$

where

$$\cos\theta = J_z/(J_x^2+J_y^2+J_z^2)^{1/2},$$
$$\sin\theta\cos\phi = J_x/(J_x^2+J_y^2+J_z^2)^{1/2},$$
$$\sin\theta\sin\phi = J_y/(J_x^2+J_y^2+J_z^2)^{1/2},$$

and $k=0$ to ∞ and $q=-k$ to k. Finally, we can condense the redundant $q\neq 0$ terms:

$$P(J,J_x,J_y,J_z) = n(J)\sum_{k,q}D(q)(2k+1)[b^k(J)]^2c(k) \times v(k)A_q^{(k)}(J)\mathrm{Re}[Y_q^{(k)}(\theta,\phi)], \quad (22)$$

where the summation over q ranges from 0 to k.

The shape of the lower order spherical harmonics are familiar since their squares give the shapes of atomic orbitals, i.e., $|Y_0^{(0)}|^2$ has the shape of the s orbital and $|Y_0^{(2)}|^2$ that of the d_{z^2}. The rank four moments correspond to g orbitals, and their shapes may not be so well known. In Figs. 7 and 8, we have presented the high J_i shapes for all the moments which affect the line intensity for linearly polarized two-photon absorption in which the probe laser is propagating along the y axis. These moments correspond to the real portion of the spherical harmonics, $Y_q^{(k)}$. It is important to note that except for the zeroth moment, all the moments have negative as well as positive lobes. Except for the zeroth moment, each moment can represent either an increase or a decrease in the two-photon absorption probability, depending on the alignment of $\mathbf{J}_i$.

C. Extraction of the ground state moments

In general, the line intensities of all the branches can be measured at several polarization angles. This appears to be the best possible way to determine the moments because the moments of the line strength are nearly identical for the O and S branches and for the P and R branches (see Figs. 3–5). It is always worth measuring one of each of these pairs of rotational branches, i.e., the O and P branches, because the moments of their line strengths are very different. For the most general case we can write an equation employing vectors and arrays which lets us use a multivariable linear least square fit to find the moments of the ground state distribution.[31] The equation describes an overdetermined system and, hence, gives an increasingly accurate measure of the moments as we increase the amount of data recorded.

For a given J_i,Λ_i,Λ_f :

Downloaded 02 Jun 2011 to 171.66.83.218. Redistribution subject to AIP license or copyright; see http://jcp.aip.org/about/rights_and_permissions

$$\begin{pmatrix} I(J_{f1},\theta_1) \\ I(J_{f2},\theta_2) \\ \cdots \\ \cdots \\ \cdots \\ I(J_{fn},\theta_n) \end{pmatrix} = \begin{pmatrix} P_0^0(J_{f1},\theta_1)P_0^2(J_{f1},\theta_1)P_1^2(J_{f1},\theta_1)P_0^4(J_{f1},\theta_1)P_1^4(J_{f1},\theta_1) \\ P_0^0(J_{f2},\theta_2)P_0^2(J_{f2},\theta_2)P_1^2(J_{f2},\theta_2)P_0^4(J_{f2},\theta_2)P_1^4(J_{f2},\theta_2) \\ \cdots \\ \cdots \\ \cdots \\ P_0^0(J_{fn},\theta_n)P_0^2(J_{fn},\theta_n)P_1^2(J_{fn},\theta_n)P_0^4(J_{fn},\theta_n)P_1^4(J_{fn},\theta_n) \end{pmatrix} \begin{pmatrix} a_0^0(\text{app}) \\ a_0^2(\text{app}) \\ a_1^2(\text{app}) \\ a_0^4(\text{app}) \\ a_1^4(\text{app}) \end{pmatrix}, \tag{23}$$

where

$$a_0^k(\text{app}) = \sum_{k',q'=\text{even}} c(k,k',q,q')a_{q'}^{k'}(J_i);$$

$$a_1^k(\text{app}) = \sum_{k',q'=odd} c(k,k',q,q')a_{q'}^{k'}(J_i), \tag{24}$$

$$a_q^k(J_i) = A_q^{(k)}(J_i)n(J_i)C(\text{det}), \tag{25}$$

$$A_q^{(k)}(J_i) = a_q^k(J_i)/a_0^0(J_i), \tag{26}$$

$$a_0^0(J_i) = n(J_i)C(\text{det}). \tag{27}$$

Here we have introduced two new quantities, the apparent moments of the ground state distribution, $a_q^k(\text{app})$, and the unreduced moments of the ground state distribution $a_q^k(J_i)$. The latter are proportional to the moments of the ground state distribution, and we can readily convert from the unreduced to the reduced moments by dividing the former by the zeroth unreduced moment. Unfortunately, we cannot directly measure the unreduced moments when the laser propagation direction is fixed, i.e., χ is constant. Under these conditions, the noncylindrically symmetric moments have line strengths which are linearly dependent upon those for the cylindrically symmetric moments, and hence the apparent moments are sums over the unreduced moments. In Table VIII, we give the expansion coefficients, $c(k,k',q,q')$ for Eq. (24) for the case $\chi = 0$.

There are only two ways to determine the individual unreduced moments: first, vary χ in order to remove the linear dependency in the line strength; second, determine the cylindrically symmetric moments at $\theta = 0$ and subtract these known values from the apparent moments to get the even q unreduced noncylindrically symmetric moments.

Recording the data at $\theta = 0°$ sets all the noncylindrically symmetric moments of the line strength equal to zero. Under these conditions, if we can record the line intensities of three of the branches, we can exactly determine the cylindrically symmetric moments of the ground state according to

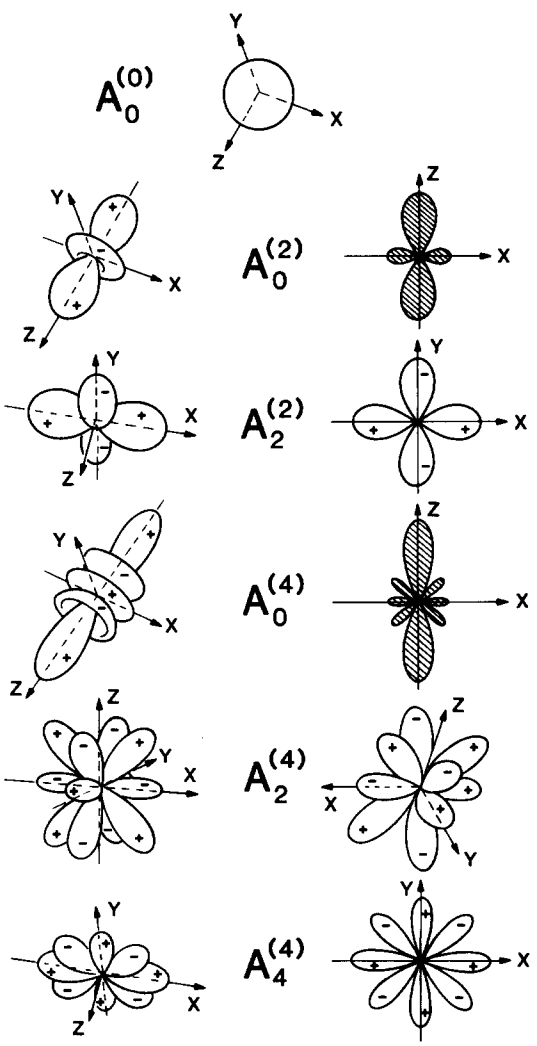

FIG. 7. Three-dimensional diagrams of the $A_q^{(k)}(J_i)$ with even components in the high J_i limit. These functions are proportional to the real parts of the corresponding spherical harmonics, $Y_q^{(k)}$.

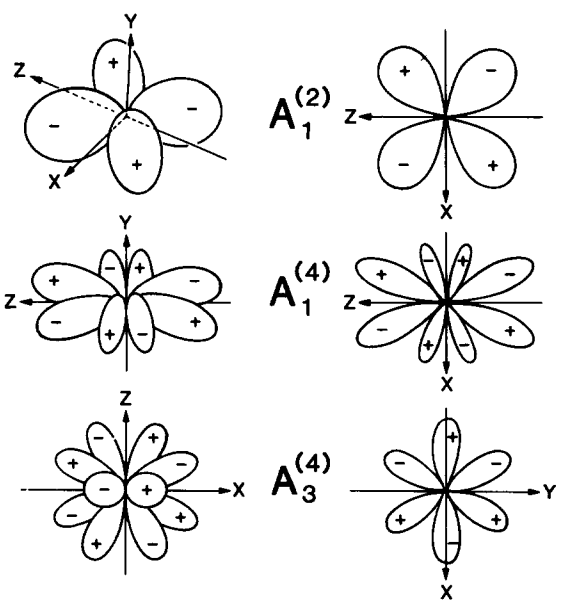

FIG. 8. Three-dimensional diagrams of the $A_q^{(k)}(J_i)$ with odd components in the high J_i limit. These functions are proportional to the real parts of the corresponding spherical harmonics, $Y_q^{(k)}$.

Downloaded 02 Jun 2011 to 171.66.83.218. Redistribution subject to AIP license or copyright; see http://jcp.aip.org/about/rights_and_permissions

TABLE VIII. The apparent moments as a function of the reduced moments of the ground state distribution for $\chi = 0$, orthogonal detection geometry.

$$a_0^0(\text{app}) = a_0^0 + 2[(5/6)^{1/2}a_2^2 + (7/10)^{1/2}a_4^4 + (1/10)^{1/2}a_2^4]$$
$$a_0^2(\text{app}) = a_0^2 + 2[-(1/6)^{1/2}a_2^2 - (2/7)^{1/2}a_4^4 + (1/2)a_2^4]$$
$$a_1^2(\text{app}) = a_1^2 + (6/7)^{1/2}a_3^4$$
$$a_0^4(\text{app}) = a_0^4 + 2[(1/70)^{1/2}a_4^4 - (2/5)^{1/2}a_2^4]$$
$$a_1^4(\text{app}) = a_1^4 - (1/7)^{1/2}a_3^4$$

$$\begin{pmatrix} I(J_{f1}) \\ I(J_{f2}) \\ I(J_{f3}) \end{pmatrix} = \begin{pmatrix} P_0^0(J_{f1}) P_0^2(J_{f1}) P_0^4(J_{f1}) \\ P_0^0(J_{f2}) P_0^2(J_{f2}) P_0^4(J_{f2}) \\ P_0^0(J_{f3}) P_0^2(J_{f3}) P_0^4(J_{f3}) \end{pmatrix} \begin{pmatrix} a_0^0 \\ a_0^2 \\ a_0^4 \end{pmatrix}. \tag{28}$$

Only three measurements suffice to determine a_0^0, a_0^2, and a_0^4; however more measurements will once again overdetermine the solution and allow a meaningful error analysis.

There is a unique set of zeroth, second, and fourth moments for any ground state distribution, but, in general, the reverse, is not true. Even though we can find the three cylindrically symmetric moments, we have not determined the $\mathbf{J}_i$ distribution. The moments we have determined could be generated by a pure combination of $A_0^{(0)}$, $A_0^{(2)}$, and $A_0^{(4)}$ terms in Eq. (19) where the other moments are set to zero.

Alternatively, there are many $\mathbf{J}_i$ distributions which have lower order moments identical to those we measured but also contain nonzero higher order moments. Only if $2J_i$ is less than or equal to the number of moments recorded can we determine completely the ground state distribution.

IV. SOME SPECIAL CASES

In this section we discuss the special cases under which the equations for the two-photon intensity can be reduced to a much simpler form. These limits serve to check the analytical formulas presented in this paper, and, more importantly, the computer programs used to analyze raw data. This section also includes a description of the experimental conditions under which only certain moments of the distribution affect the recorded line intensities, i.e., the "magic angles" for two-photon absorption. We also discuss how to take $2+1$ LIF data in which the fluorescence has been averaged over its spatial anisotropy.

A. The BH factors

The line strengths for two-photon absorption by diatomic molecules through a virtual state from an isotropic ground state were derived by Bray and Hochstrasser.[6] We refer to these two-photon line strengths, apart from the transition dipole factor (see BH), as the Bray–Hochstrasser factors, and denote them by $\mathrm{BH}(J_i,J_f;\Delta\Lambda)$. Our intensity formulas, Eqs. (3) and (4), can be integrated analytically to give expressions $P_0^0(J_i,J_f;\Delta\Lambda)$ which are identical with the Bray–Hochstrasser factors, except for a normalization constant:

$$P_0^0(J_i,J_f;\Delta\Lambda=1) = K_0\,\mathrm{BH}(J_i,J_f;\Delta\Lambda=1)\mu^2_{\Delta\Lambda=\pm1}, \tag{29a}$$

$$P_0^0(J_i,J_f;\Delta\Lambda=2) = K_0\,\mathrm{BH}(J_i,J_f;\Delta\Lambda=2)\mu^2_{\Delta\Lambda=\pm2}, \tag{29b}$$

$$P_0^0(J_i,J_f;\Delta\Lambda=0) = K_0[\mathrm{BH}_i(J_i,J_f;\Delta\Lambda=0)\mu_i^2 + \mathrm{BH}_s(J_i,J_f;\Delta\Lambda=0)\mu_s^2], \tag{29c}$$

where

$$K_0 = (4\pi/3)^2(2J_i+1)^{-1}, \tag{30}$$

$$\mu^2_{\Delta\Lambda=\pm1} = |\mu_\parallel\mu_\pm + \mu'_\pm\mu'_\parallel|^2 = |R^0_{ei}R^{\pm1}_{fe} + R^{\pm1}_{ei}R^0_{fe}|^2, \tag{31a}$$

$$\mu^2_{\Delta\Lambda=\pm2} = |\mu_\pm\mu'_\pm|^2 = |R^{\pm1}_{ei}R^{\pm1}_{fe}|^2, \tag{31b}$$

$$\mu_i^2 = |\mu_\parallel\mu'_\parallel - \mu_+\mu'_- - \mu''_-\mu''_+|^2 = |R^0_{ei}R^0_{fe} - R^{+1}_{ei}R^{-1}_{fe} - R^{-1}_{ei}R^{+1}_{fe}|^2, \tag{31c}$$

$$\mu_s^2 = |2\mu_\parallel\mu'_\parallel + \mu_+\mu'_- + \mu''_-\mu''_+|^2 = |2R^0_{ei}R^0_{fe} + R^{+1}_{ei}R^{-1}_{fe} + R^{-1}_{ei}R^{+1}_{fe}|^2. \tag{31d}$$

Here, the $\mu_{\Delta\Lambda}$, μ_s, and μ_i are the total transition dipole moments as defined with our definitions of the raising and lowering dipole moment operators. The $\mu_\parallel$ and $\mu_\pm$ are equivalent to the $R_{21}^{(\Lambda_2-\Lambda_1)}$, the radial portions of the transition dipole moment integral, where the subscripts on μ refer to the change in Λ for the single-photon transition and the primes refer to the different pathways (see BH). The subscripts on R indicate the step, e.g., $R_{ei}^{(\Lambda_e-\Lambda_i)}$ refers to the transition from the initial to excited state, and $R_{fe}^{(\Lambda_f-\Lambda_e)}$ refers to the transition from the excited to the final state. Normally, we set all the $R_{21}^{(\Lambda_2-\Lambda_1)}$ equal to unity. This does not really matter except for the Q branch of a transition in which $\Lambda_i = \Lambda_f$. For this case, the above assumptions determine the value of the two independent transition dipole moments in the BH treatment, μ_s and μ_i.

Bray and Hochstrasser[6] explicitly define their tensor moments as $\mu_\pm = (1/2)^{1/2}(\mu_x \pm i\mu_y)$; this is an anomalous convention. We instead use the standard convention for a first-rank tensor,[26–30] namely, $\mu_\pm = \mp(1/2)^{1/2}(\mu_x \pm i\mu_y)$. Hence when comparing our formulas for the total transition moments with those of BH, it seems that the μ_+ had been replaced by $-\mu_+$. This affects the values of μ_i and μ_s, and hence the interpretation of the parallel vs perpendicular character of a $\Delta\Lambda = 0$ two-photon transition for which μ_s and μ_i have been measured.[32]

In Table IX we present the Bray–Hochstrasser factors with our normalization for all possible two-photon transitions. Please note that there was a typographical error in BH for the appropriate factor for the P branch of a $\Lambda_f = \Lambda_i \pm 1$ transition.

B. Correspondence with GZ results

By setting $J'_e = J_e$, $\Lambda'_e = \Lambda_e$, and $q = 0$ in Eqs. (3) and (4), we recover the expression Greene and Zare derived for $1+1$ LIF. More importantly, these assumptions also force our equations for S, h, and ϵ to equal those of GZ. For example, if $\theta = 0°$, the $\epsilon(k_d,k_a,k,0;\Omega)$ are identical with those for case 1 in Table II of GZ.

Downloaded 02 Jun 2011 to 171.66.83.218. Redistribution subject to AIP license or copyright; see http://jcp.aip.org/about/rights_and_permissions

TABLE IX. The Bray–Hochstrasser factors with the normalization of this paper. For states with no electron or nuclear spin degeneracy, these factors are equal to P_0^0 and are equivalent to the two-photon transition strengths when the ground state is isotropic. In this table, $J = J_i$, i.e., J refers to the angular momentum quantum number of the ground state. All the $\Delta\Lambda = \pm 1$ entries have a transition dipole factor of $\mu^2_{\Delta\Lambda=\pm 1}$ while the $\Delta\Lambda = \pm 2$ entries employ $\mu^2_{\Delta\Lambda=\pm 2}$ and the $\Delta\Lambda = 0$ entries employ μ_s^2 except for the Q branch of a $\Delta\Lambda = 0$ transition. The entries are for excitation by linearly polarized light. The transition strengths for circularly polarized light are obtained by multiplying the values by 3/2 except for the Q branch of a $\Delta\Lambda = 0$ transition branch; it has the value $(2J+1)[J(J+1) - 3\Lambda^2]^2/[30J(J+1)(2J+3)(2J-1)]$.

$\Delta\Lambda = \pm 2$

O branch:

$$\frac{K_0(J \mp \Lambda)(J \mp \Lambda - 1)(J \mp \Lambda - 2)(J \mp \Lambda - 3)}{30J(J-1)(2J-1)}$$

P branch:

$$\frac{K_0(J \mp \Lambda)(J \mp \Lambda - 1)(J \mp \Lambda - 2)(J \pm \Lambda + 1)}{15J(J+1)(J-1)}$$

Q branch:

$$\frac{K_0(J \mp \Lambda)(J \mp \Lambda - 1)(J \pm \Lambda + 1)(J \pm \Lambda + 2)(2J+1)}{5J(J+1)(2J-1)(2J+3)}$$

R branch:

$$\frac{K_0(J \mp \Lambda)(J \pm \Lambda + 1)(J \pm \Lambda + 2)(J \pm \Lambda + 3)}{15J(J+1)(J+2)}$$

S branch:

$$\frac{K_0(J \pm \Lambda + 1)(J \pm \Lambda + 2)(J \pm \Lambda + 3)(J \pm \Lambda + 4)}{30(J+1)(J+2)(2J+3)}$$

$\Delta\Lambda = \pm 1$

$$\frac{K_0(J \mp \Lambda - 1)(J \mp \Delta)(J \mp \Lambda - 2)(J \pm \Lambda)}{15J(J-1)(2J-1)}$$

$$\frac{K_0(J \mp \Lambda - 1)(J \mp \Lambda)(J \pm 2\Lambda + 1)^2}{30J(J+1)(J-1)}$$

$$\frac{K_0(J \pm \Lambda + 1)(2\Lambda \pm 1)^2(2J+1)(J \mp \Lambda)}{10J(J+1)(2J-1)(2J+3)}$$

$$\frac{K_0(J \pm \Lambda + 1)(J \pm \Lambda + 2)(J \mp 2\Lambda)^2}{30J(J+1)(J+2)}$$

$$\frac{K_0(J \pm \Lambda + 1)(J \pm \Lambda + 2)(J \pm \Lambda + 3)(J \mp \Lambda + 1)}{15(J+1)(J+2)(2J+3)}$$

$\Delta\Lambda = 0$

O branch: $$\frac{K_0(J^2 - \Lambda^2)[(J-1)^2 - \Lambda^2]}{30J(J-1)(2J-1)}\mu_s^2$$

P branch: $$\frac{2K_0\Lambda^2(J^2 - \Lambda^2)}{30J(J+1)(J-1)}\mu_s^2$$

Q branch: $$\frac{K_0(2J+1)}{9}\mu_i^2 + \frac{K_0(2J+1)[J(J+1) - 3\Lambda^2]^2}{45J(J+1)(2J-1)(2J+3)}\mu_s^2$$

R branch: $$\frac{2K_0\Lambda^2[(J+1)^2 - \Lambda^2]}{30J(J+1)(J+2)}\mu_s^2$$

S branch: $$\frac{K_0[(J+1)^2 - \Lambda^2][(J+2)^2 - \Lambda^2]}{30(J+1)(J+2)(2J+3)}\mu_s^2$$

where

$K_0 = (4\pi/3)^2(2J_i + 1)^{-1}$

$\mu^2_{\Delta\Lambda=\pm 1} = |\mu_\parallel \mu_\pm + \mu'_\pm \mu'_\parallel|^2 = |R^0_{ei} R^{\pm 1}_{fe} + R^{\pm 1}_{ei} R^0_{fe}|^2$

$\mu^2_{\Delta\Lambda=\pm 2} = |\mu_\pm \mu'_\pm|^2 = |R^{\pm 1}_{ei} R^{\pm 1}_{fe}|^2$

$\mu_i^2 = |\mu_\parallel \mu'_\parallel - \mu_+ \mu'_- - \mu''_- \mu''_+|^2 = |R^0_{ei} R^0_{fe} - R^{+1}_{ei} R^{-1}_{fe} - R^{-1}_{ei} R^{+1}_{fe}|^2$

$\mu_s^2 = |2\mu_\parallel \mu'_\parallel + \mu_+ \mu'_- + \mu''_- \mu''_+|^2 = |2R^0_{ei} R^0_{fe} + R^{+1}_{ei} R^{-1}_{fe} + R^{-1}_{ei} R^{+1}_{fe}|^2$

C. Magic angles

In contrast to LIF, magic angles are very easy to utilize in single-color two-photon absorption spectroscopy. In LIF we must separately consider the geometry of the polarization vectors of both the absorbed and detected photons; hence in order to get a magic angle we must specify two sets of angles. In two-photon absorption spectroscopy, the photons are identical; hence, magic angles can be reached solely by specifying θ, the angle of the laser polarization vector if the laser propagation vector lies in the x–y plane of the lab frame.

At $\theta = 0°$ all the $P^k_{q\neq 0}$ vanish and at $\theta = 90°$ all the $P^k_{q=\text{odd}}$ vanish since the corresponding spherical harmonics in the equation for $\epsilon(k_d, k_a, k, q; \Omega)$ are zero. As previously mentioned, we can determine the cylindrically symmetric moments at $\theta = 0°$ using the intensities of three or more rotational branches.

At $\theta = 54.7°$, P_0^2 vanishes. Thus if we can assume cylindrical symmetry, we can determine $n(J_i)$ and $A_0^{(4)}(J_i)$ from the line intensities of just two rotational branches.[33]

At both $\theta = 30.6°$ and $70.1°$, P_0^4 vanishes. Thus if we can assume cylindrical symmetry, we can detemrine $n(J_i)$ and $A_0^{(2)}(J_i)$ from the line intensities of just two rotational branches.

At $\theta = 67.8°$ P_2^4 equals zero and at $\theta = 49.1°$ P_1^4 vanishes. These facts do not have much importance experimental-

Downloaded 02 Jun 2011 to 171.66.83.218. Redistribution subject to AIP license or copyright; see http://jcp.aip.org/about/rights_and_permissions

ly, but they do serve as a nice check on the numerically calculated values of P_2^4 and P_1^4.

For a cylindrically symmetric ground state distribution we only need to vary the angle of the polarizer once to determine all the measurable moments, $n(J_i)$, $A_0^{(2)}(J_i)$, $A_0^{(4)}(J_i)$: one spectrum must be recorded at $\theta = 54.7°$ and another at either $\theta = 30.6°$ or 70.1°.

D. 2+1 LIF

In order to apply Eqs. (3) and (4) for 2 + 1 LIF, the fluorescence must be collected independent of its polarization and anisotropy. The former is easily accomplished, but, in general, the latter requirement is difficult to fulfill without moving the fluorescence detector or capturing a large solid angle element of the fluorescence. However, when the distribution is known to have cylindrical symmetry, such as in photolysis, then it may be possible to vary the symmetry axis in a manner which averages the spatial anisotropy of the radiation.

V. CONCLUDING REMARKS

We have presented a completely general formalism for determining populations and alignments for single-color two-photon absorption spectroscopy utilizing linearly polarized light. All the formulas have been summarized in Tables I–V, and these tables can be used directly to reduce two-photon absorption spectra into populations and alignments. This is only half the story; the $\mathbf{J}_i$ distribution may not only be aligned, but also oriented, i.e., it may have a net helicity. In order to detect this orientation, the two-photon absorption must be carried out using circularly or elliptically polarized light. We have extended the analysis presented in this paper so that the orientation moments can also be extracted.[34] The formulas presented in this paper have been used to analyze the $\mathbf{J}_i$ distribution of N_2 scattered from a clean single-crystal Ag(111) surface, and the results of this are described in a subsequent publication.[35]

ACKNOWLEDGMENTS

We would like to thank C. H. Greene, M. A. O'Halloran, D. C. Jacobs, H. Joswig, and the J. Vigué for many useful discussions. We are greatly indebted to K.-D. Rinnen for proofreading this manuscript. The computations were performed at the Stanford Cell Biology Computer Center under N.S.F. DMB 84-00396 with the assistance of D. E. Austen. We would also like to acknowledge the assistance of J. Choi and W. E. Conaway in preparing the figures. This work was supported by the Office of Naval Research under N00014-78-C-0403 and the Army Research Office under DAAG-29-84-K-0027.

APPENDIX

We consider here the derivation of the expressions appearing in Tables I–IV. The Appendix is divided into seven parts. First we factor the equation for two-photon absorption into a geometric term, an angular momentum coupling term, and a reduced matrix element of the spherical tensor angular momentum operator (Sec. 1). Second, we reduce the angular momentum term to the product of a 6-j symbol, a 9-j symbol, and reduced matrix elements of the dipole moment operator (Sec. 2). Third, we evaluate the reduced matrix elements of the dipole operator for singlet states (Sec. 3). Fourth, we simplify the geometric term involving the excitation–detection scheme to a form containing only a single spherical harmonic (Sec. 4). Fifth, we present the hyperfine and spin depolarization factors (Sec. 5). Sixth, we calculate the matrix elements of the spherical tensor angular momentum operator and combine them so as to have only real matrix elements (Sec. 6). Seventh, we present the simplified case for orthogonal excitation/detection geometry (Sec. 7). Care has been taken to show intermediate steps in these derivations so that this treatment can be extended to more complex cases. We rely extensively on the angular momentum machinery presented in Edmonds[29] and cite his equations as E. followed by his equation numbers.

1. Factorization of the two-photon absorption equation

The starting equation for the time-independent two-photon absorption probability was given in Sec. II:

$$I = C \sum_{M_f} \left\langle \left| \sum_{\substack{J_e M_e \Lambda_e \\ \gamma_e}} \frac{(J_f, M_f, \Lambda_f | \hat{\mathbf{e}}_d \cdot \mathbf{r}_1 | \gamma_e, J_e, M_e, \Lambda_e)(\gamma_e, J_e, M_e, \Lambda_e | \hat{\mathbf{e}}_a \cdot \mathbf{r}_2 | J_i, M_i, \Lambda_i)}{E_{ei} - h\nu + i(\Gamma_e/2)} \right|^2 \right\rangle . \tag{A1}$$

This equation is analogous to Eq. (27) of GZ and the definitions of the terms are identical. For the sake of brevity we have omitted electronic and vibronic state quantum numbers, but they will be explicitly written out when evaluating the radial portion of the dipole moment matrix elements. Here, $\hat{\mathbf{e}}_a$ and $\hat{\mathbf{e}}_d$ are the polarization unit vectors of the first and second photons, and $\mathbf{r}$ is the dipole moment operator. The constant C is proportional to the total population in state J_i, Λ_i and also embodies various normalization factors. The brackets $\langle\ \rangle$ indicate a weighted average over all M_i. Hence our intensity expression differs from that of BH by a factor proportional to $(2J_i + 1)$. We expand the square in Eq. (A1):

$$I = C \sum_{M_f} \left\langle \sum_{\substack{\gamma'_e, J'_e, M'_e, \Lambda'_e \\ \gamma_e, J_e, M_e, \Lambda_e}} (J_i M_i \Lambda_i | \hat{\mathbf{e}}_a^* \cdot \mathbf{r}_1 | \gamma'_e J'_e M'_e \Lambda'_e)(\gamma'_e J'_e M'_e \Lambda'_e | \hat{\mathbf{e}}_d^* \cdot \mathbf{r}_2 | J_f M_f \Lambda_f)/ \right.$$
$$\left. D'_{ei} (J_f M_f \Lambda_f | \hat{\mathbf{e}}_d \cdot \mathbf{r}_3 | \gamma_e J_e M_e \Lambda_e)(\gamma_e J_e M_e \Lambda_e | \hat{\mathbf{e}}_a \cdot \mathbf{r}_4 | J_i M_i \Lambda_i)/D_{ei} \right\rangle , \tag{A2}$$

where D_{ei} and D'_{ei} are the energy denominators from Eq. (A1). Next, we identify the projection operators:

Downloaded 02 Jun 2011 to 171.66.83.218. Redistribution subject to AIP license or copyright; see http://jcp.aip.org/about/rights_and_permissions

$$P_e = \sum_{\gamma_e, J_e, M_e, \Lambda_e} |\gamma_e J_e M_e \Lambda_e)(\gamma_e J_e M_e \Lambda_e|, \tag{A3a}$$

$$P'_e = \sum_{\gamma'_e, J'_e, M'_e, \Lambda'_e} |\gamma'_e J'_e M'_e \Lambda'_e)(\gamma'_e J'_e M'_e \Lambda'_e|, \tag{A3b}$$

$$P_f = \sum_{M_f} |J_f M_f \Lambda_f)(J_f M_f \Lambda_f|, \tag{A3c}$$

and insert them into Eq. (A2). This is advantageous because they are scalars (tensors of rank $k = 0$) and hence readily commute with each other and with other scalars:

$$I = C\langle (J_i M_i \Lambda_i | (\hat{\mathbf{e}}_a^* \cdot \mathbf{r}_1) P'_e (\hat{\mathbf{e}}_d^* \cdot \mathbf{r}_2) P_f (\hat{\mathbf{e}}_d \cdot \mathbf{r}_3) P_e (\hat{\mathbf{e}}_a \cdot \mathbf{r}_4) | J_i M_i \Lambda_i) \rangle. \tag{A4}$$

This equation is identical with Eq. (30) of GZ. However our projection operators are different than those of GZ because our excited state does not have a unique J_e or Λ_e. Next, we follow the FM approach and separate the angular momentum coupling factors from the geometric factors. This has already been done for the above equation by GZ. From Eqs. (41), (42), and (48) of GZ, it follows that

$$I = C \sum_{k_d, k_a, k, q} (-1)^{k-q} \epsilon_q^{(k)}(k_d, k_a; \Omega) \langle (J_i M_i \Lambda_i | J^{(k)}_{-q} | J_i M_i \Lambda_i) \rangle Z / (J_i \| J^{(k)} \| J_i), \tag{A5}$$

where

$$Z = (J_i \| \{ [r_2^{(1)} \times r_3^{(1)}]^{(k_d)} [r_1^{(1)} \times r_4^{(1)}]^{(k_a)} \}^{(k)} P'_e P_f P_e \| J_i), \tag{A6}$$

$$\epsilon_q^{(k)}(k_d, k_a; \Omega) = \{ [e_d^{*(1)} \times e_d^{(1)}]^{(k_d)} \times [e_a^{*(1)} \times e_a^{(1)}]^{(k_a)} \}_q^{(k)}. \tag{A7}$$

The superscript (k) and subscript q on $\epsilon_q^{(k)}$ are employed to indicate that ϵ is a spherical tensor operator; this notation differs only in appearance from that of GZ.

2. The angular momentum coupling factors

Our first task is to simplilfy Z. We substitute the expressions for the projection operators, Eqs. (A3a), (A3b), and (A3c), into Eq. (A6):

$$\begin{aligned} Z = & \sum_{\substack{q_d, q_a, q, M_f \\ q_1, q_2, q_3, q_4}} \sum_{\substack{\gamma'_e, J'_e, M'_e, \Lambda'_e, M'_i \\ \gamma_e, J_e, M_e, \Lambda_e, \Lambda_i}} (J_i M_i \Lambda_i | r_{q_1}^{(1)} | \gamma'_e J'_e M'_e \Lambda'_e) \\ & \times (\gamma'_e J'_e M'_e \Lambda'_e | r_{q_2}^{(1)} | J_f M_f \Lambda_f)(J_f M_f \Lambda_f | r_{q_3}^{(1)} | \gamma_e J_e M_e \Lambda_e)(\gamma_e J_e M_e \Lambda_e | r_{q_4}^{(1)} | J_i M'_i \Lambda_i) / D_{ei} D_{ei}^{*\prime} \\ & \times (1q_2, 1q_3 | k_d q_d)(1q_1, 1q_4 | k_a q_a)(k_d q_d, k_a q_a | kq)(-1)^{(J_i - M_i)} \begin{pmatrix} J_i & k & J_i \\ -M_i & q & M'_i \end{pmatrix}. \end{aligned} \tag{A8}$$

We apply the Wigner–Eckart theorem (E.5.4.1) to the four matrix elements, and we convert the three Clebsch–Gordan coefficients to 3-j symbols (E.3.7.3):

$$\begin{aligned} Z = & \sum_{\substack{\text{all } q, M \\ \gamma'_e, J'_e, \Lambda'_e, \gamma_e, J_e, \Lambda_e}} (-1)^{(J_i - M_i)} \begin{pmatrix} J_i & 1 & J'_e \\ -M_i & q_1 & M'_e \end{pmatrix} (J_i \Lambda_i \| r^{(1)} \| \gamma'_e J'_e \Lambda'_e) \\ & \times (-1)^{(J'_e - M'_e)} \begin{pmatrix} J'_e & 1 & J_f \\ -M'_e & q_2 & M_f \end{pmatrix} (\gamma'_e J'_e \Lambda'_e \| r^{(1)} \| J_f \Lambda_f) \\ & \times (-1)^{(J_f - M_f)} \begin{pmatrix} J_f & 1 & J_e \\ -M_f & q_3 & M_e \end{pmatrix} (J_f \Lambda_f \| r^{(1)} \| \gamma_e J_e \Lambda_e) (-1)^{(J_e - M_e)} \begin{pmatrix} J_e & 1 & J_i \\ -M_e & q_4 & M'_i \end{pmatrix} (\gamma_e J_e \Lambda_e \| r^{(1)} \| J_i \Lambda_i) \\ & \times (2k_d + 1)^{1/2} (-1)^{-q_d} \begin{pmatrix} 1 & 1 & k_d \\ q_2 & q_3 & -q_d \end{pmatrix} (2k_a + 1)^{1/2} (-1)^{-q_a} \begin{pmatrix} 1 & 1 & k_a \\ q_1 & q_4 & -q_a \end{pmatrix} \\ & \times (2k + 1)^{1/2} (-1)^{(k_a - k_d - q)} \begin{pmatrix} k_d & k_a & k \\ q_d & q_a & -q \end{pmatrix} (-1)^{(J_i - M_i)} \begin{pmatrix} J_i & k & J_i \\ -M_i & q & M'_i \end{pmatrix} \Big/ D_{ei} D_{ei}^{*\prime}. \end{aligned} \tag{A9}$$

We simplify the phase factors by noting that k and all q are integers while all J and M are either integers or half-integers.

Downloaded 02 Jun 2011 to 171.66.83.218. Redistribution subject to AIP license or copyright; see http://jcp.aip.org/about/rights_and_permissions

This allows us to flip the signs of k, all q, all $2J$, and all $2M$ that appear in the phase factors; for example $(-1)^{(M_i - M_f)} = (-1)^{(M_f - M_i)}$. We also use the following relationships:

$$M'_e = q_2 + M_f, \tag{A10a}$$

$$M_e = M_f - q_3, \tag{A10b}$$

$$q = q_a + q_d, \tag{A10c}$$

which ensure that the corresponding 3-j symbols in Eq. (A9) do not vanish.

In addition we perform a few symmetry operations on the 3-j symbols in order to simplify their contraction into a 6-j symbol (E.3.7.4–6). These operations do not introduce any new phase factors.

$$Z = \sum_{\substack{\text{all } q,M \\ J_e \Lambda_e J'_e \Lambda'_e}} (-1)^{(-J'_e - J_f - J_e + k_a - k_d)} (-1)^{(q_2 - q_3 - M_f)} [(2k_d+1)(2k_a+1)(2k+1)]^{1/2}$$

$$\times \begin{pmatrix} J'_e & 1 & J_f \\ -M'_e & q_2 & M_f \end{pmatrix} \begin{pmatrix} 1 & J_e & J_f \\ q_3 & M_e & -M_f \end{pmatrix} \begin{pmatrix} 1 & 1 & k_d \\ -q_3 & -q_2 & q_d \end{pmatrix} \begin{pmatrix} J_i & 1 & J'_e \\ -M_i & q_1 & M'_e \end{pmatrix}$$

$$\times \begin{pmatrix} J_e & 1 & J_i \\ -M_e & q_4 & M_i \end{pmatrix} \begin{pmatrix} k_d & k_a & k \\ -q_d & q_a & -q \end{pmatrix} \begin{pmatrix} J_i & k & J_i \\ -M_i & q & M_i \end{pmatrix} \begin{pmatrix} 1 & 1 & k_a \\ q_1 & q_4 & -q_a \end{pmatrix}$$

$$\times s(J_i, \Lambda_i, J_e, \Lambda_e, J'_e \Lambda'_e, J_f, \Lambda_f), \tag{A11a}$$

where

$$s(J_i, \Lambda_i, J_e, \Lambda_e J'_e, \Lambda'_e, J_f, \Lambda_f) = \sum_{\gamma_e \gamma'_e} (J_i \Lambda_i \| r^{(1)} \| \gamma'_e J'_e \Lambda'_e)(\gamma'_e J'_e \Lambda'_e \| r^{(1)} \| J_f \Lambda_f) / D^{*\prime}_{ei}$$

$$\times (J_f \Lambda_f \| r^{(1)} \| \gamma_e J_e \Lambda_e)(\gamma_e J_e \Lambda_e \| r^{(1)} \| J_i \Lambda_i) / D_{ei}. \tag{A11b}$$

We can perform the summation over M_f, q_2, and q_3 using only the second phase factor and the first three 3-j symbols by employing the identity (E.6.2.8):

$$\sum_{M_f, q_2, q_3} (-1)^{(q_2 - q_3 - M_f)} \begin{pmatrix} J'_e & 1 & J_f \\ -M'_e & q_2 & M_f \end{pmatrix} \begin{pmatrix} 1 & J_e & J_f \\ q_3 & M_e & -M_f \end{pmatrix} \begin{pmatrix} 1 & 1 & k_d \\ -q_3 & -q_2 & q_d \end{pmatrix}$$

$$= (-1)^{-J_f} \begin{pmatrix} J'_e & J_e & k_d \\ -M'_e & M_e & q_d \end{pmatrix} \begin{Bmatrix} J'_e & J_e & k_d \\ 1 & 1 & J_f \end{Bmatrix}. \tag{A12}$$

We substitute Eq. (A12) into Eq. (A11) and simplify the remaining phase factor; this is the first phase factor in the equation below. Next, we perform a few symmetry operations on the remaining 3-j symbols (E.3.7.4–6) in order to convert them into a form which is easy to contract into a 9-j symbol; this generates the second phase factor in the equation below:

$$Z = \sum_{J_e \Lambda_e J'_e \Lambda'_e} (-1)^{(-J'_e - 2J_f - J_e + k_a - k_d)} [(2k_d+1)(2k_a+1)(2k+1)]^{1/2} \begin{Bmatrix} J'_e & J_e & k_d \\ 1 & 1 & J_f \end{Bmatrix}$$

$$\times \sum_{\substack{M_i M_e M'_i M'_e \\ q_1 q_4 q_a q_d}} (-1)^{(1 - J_i + k - J'_e + k_d)} \begin{pmatrix} J_i & 1 & J'_e \\ -M_i & q_1 & M'_e \end{pmatrix} \begin{pmatrix} J_i & 1 & J_e \\ M'_i & q_4 & -M_e \end{pmatrix}$$

$$\times \begin{pmatrix} k & k_a & k_d \\ q & -q_a & -q_d \end{pmatrix} \begin{pmatrix} J_i & J_i & k \\ -M_i & M'_i & q \end{pmatrix} \begin{pmatrix} 1 & 1 & k_a \\ q_1 & q_4 & -q_a \end{pmatrix} \begin{pmatrix} J'_e & J_e & k_d \\ M'_e & -M_e & -q_d \end{pmatrix}$$

$$\times s(J_i, \Lambda_i, J_e, \Lambda_e, J'_e, \Lambda'_e, J_f, \Lambda_f). \tag{A13}$$

In the above equation none of the indices in the second summation appear in the phase factors. Thus, the summation of six 3-j symbols in Eq. (A13) reduces to a single 9-j symbol (E.6.4.4). We then use the symmetry properties of the 9-j symbol to convert it to a form analogous to that derived by GZ (E.6.4.5):

Downloaded 02 Jun 2011 to 171.66.83.218. Redistribution subject to AIP license or copyright; see http://jcp.aip.org/about/rights_and_permissions

$$\sum_{\substack{M_i,M_e,M_i',M_e' \\ q_1,q_4,q_a,q_d}} \begin{pmatrix} J_i & 1 & J_e' \\ -M_i & q_1 & M_e' \end{pmatrix} \begin{pmatrix} J_i & 1 & J_e \\ M_i' & q_4 & -M_e \end{pmatrix}$$

$$\times \begin{pmatrix} k & k_a & k_d \\ q & -q_a & -q_d \end{pmatrix} \begin{pmatrix} J_i & J_i & k \\ -M_i & M_i' & q \end{pmatrix} \begin{pmatrix} 1 & 1 & k_a \\ q_1 & q_4 & -q_a \end{pmatrix} \begin{pmatrix} J_e' & J_e & k_d \\ M_e' & -M_e & -q_d \end{pmatrix}$$

$$= \begin{Bmatrix} J_i & 1 & J_e' \\ J_i & 1 & J_e \\ k & k_a & k_d \end{Bmatrix} = (-1)^{(2J_i + J_e' + J_e + k + k_a + k_d)} \begin{Bmatrix} J_e' & 1 & J_i \\ J_e & 1 & J_i \\ k_d & k_a & k \end{Bmatrix}. \tag{A14}$$

By substituting Eq. (A14) into Eq. (A13) and combining the phase factor of Eq. (A14) with the second phase factor of Eq. (A13) we derive

$$Z = \sum_{J_e',\Lambda_e',J_e,\Lambda_e} (-1)^{(J_e + k_a + 1 + J_i)} (-1)^{(-J_e' - 2J_f - J_e + k_a - k_d)} [(2k_d + 1)(2k_a + 1)(2k + 1)]^{1/2}$$

$$\times \begin{Bmatrix} J_e' & J_e & k_d \\ 1 & 1 & J_f \end{Bmatrix} \begin{Bmatrix} J_e' & 1 & J_i \\ J_e & 1 & J_i \\ k_d & k_a & k \end{Bmatrix} s(J_i,\Lambda_i,J_e,\Lambda_e,J_e',\Lambda_e',J_f,\Lambda_f). \tag{A15}$$

We rewrite the reduced matrix elements appearing in $s(J_i,\Lambda_i,J_e,\Lambda_e,J_e',\Lambda_e',J_f,\Lambda_f)$ so that it is a positive definite quantity when the virtual state is replaced by a real state [see Eq. (54) of GZ]. Toward this end, we convert two of the reduced matrix elements to their respective complex conjugates:

$$(J_i\Lambda_i\|r^{(1)}\|\gamma_e'J_e'\Lambda_e') = (-1)^{(J_e' - J_i)} (\gamma_e'J_e'\Lambda_e'\|r^{(1)}\|J_i\Lambda_i)^*, \tag{A16}$$

$$(\gamma_e'J_e'\Lambda_e'\|r^{(1)}\|J_f\Lambda_f) = (-1)^{(J_f - J_e')} (J_f\Lambda_f\|r^{(1)}\|\gamma_e'J_e'\Lambda_e')^*. \tag{A17}$$

Substituting Eqs. (A16) and (A17) into Eq. (A15) and making appropriate phase factor simplifications, we find

$$Z = \sum_{J_e,\Lambda_e,J_e',\Lambda_e'} (-1)^{(J_f + J_e' - k_d + 1)} [(2k_d + 1)(2k_a + 1)(2k + 1)]^{1/2} \begin{Bmatrix} J_e' & J_e & k_d \\ 1 & 1 & J_f \end{Bmatrix}$$

$$\times \begin{Bmatrix} J_e' & 1 & J_i \\ J_e & 1 & J_i \\ k_d & k_a & k \end{Bmatrix} S(J_i,\Lambda_i,J_e,\Lambda_e,J_e',\Lambda_e',J_f,\Lambda_f), \tag{A18}$$

where

$$S(J_i,\Lambda_i,J_e,\Lambda_e,J_e',\Lambda_e',J_f,\Lambda_f) = (J_e'\Lambda_e'\|r^{(1)}\|J_i\Lambda_i)^*(J_e\Lambda_e\|r^{(1)}\|J_i\Lambda_i)(J_f\Lambda_f\|r^{(1)}\|J_e'\Lambda_e')^*(J_f\Lambda_f\|r^{(1)}\|J_e\Lambda_e). \tag{A19}$$

We have omitted the energy denominators and sums over electronic quantum numbers in Eq. (A19) because we will incorporate them into the radial portions of the reduced matrix elements. The altered reduced matrix elements are differentiated by not having electronic quantum numbers included in their arguments.

3. Calculation of the reduced matrix elements of the dipole moment operator for singlet states

The reduced matrix elements of the dipole moment operator are easily calculated from the matrix elements of the dipole moment operator using the Wigner–Eckart theorem (E.5.4.1). We are free to choose any component, q, of the matrix elements. For the sake of simplicity we let $q = 0$. Since we are interested in the dipole moment operator, we let $k = 1$. We can invert the Wigner–Eckart theorem while noting that the total sign of the phase factor can be reversed since the sum of all the terms in the phase factor is an integer:

$$(J_2\Lambda_2\|r^{(1)}\|J_1\Lambda_1) = \frac{(-1)^{(J_2 - M_2)} (J_2M_2\Lambda_2|r_0^{(1)}|J_1M_1\Lambda_1)}{\begin{pmatrix} J_2 & 1 & J_1 \\ -M_2 & 0 & M_1 \end{pmatrix}}. \tag{A20}$$

To calculate the matrix elements of the dipole moment operator we follow the procedure of Dixit and McKoy,[36] but we employ the standard phase convention for the rotational wave function, and we use the corresponding standard equation the transformation between the space-fixed and molecule-fixed frames of reference, as given by Brown and How-

Downloaded 02 Jun 2011 to 171.66.83.218. Redistribution subject to AIP license or copyright; see http://jcp.aip.org/about/rights_and_permissions

ard (BrHd).[37] These conventions[37–39] are in agreement with Brink and Satchler (BS),[30] but differ from those of Edmonds.[29] We start by writing out the wave function in the Born–Oppenheimer approximation using Eq. (17) of BrHd:

$$|\gamma v J M \Lambda) = \Psi_\gamma^{(e)}(\{\mathbf{r}_i'\};R)\chi_v(R) \times[(2J+1)/8\pi^2]^{1/2} D_{M\Lambda}^{(J)*}(\hat{R}). \quad \text{(A21)}$$

Here $\Psi_\gamma^{(e)}(\{\mathbf{r}_i'\};R)$ is the electronic wave function of state γ that depends on the positions of all the electrons in the molecular frame of reference, $\{\mathbf{r}_i'\}$, and the internuclear separation, R; $\chi_v(R)$ is the vibrational wave function for state v and also depends on the internuclear distance; and $D_{M\Lambda}^{(J)*}(\hat{R})$ is the complex conjugate of a rotation matrix coefficient as defined by BS where $\hat{R}$ denotes the Euler angles relating the space-fixed and molecule-fixed frames of reference (where Z in the molecule-fixed frame lies along J). In calculating the matrix element of $r_0^{(1)}$, we must recognize that it is expressed in the space-fixed frame of reference since in our original intensity expression, Eq. (A2), it was multiplied by another space-fixed vector, the polarization vector of the laser. In order to evaluate the matrix element of the dipole moment, we reexpress the dipole moment in the molecule-fixed frame of reference since the wave functions are expressed in terms of the molecular coordinates. Using Eq. (5) of BrHd:

$$r_0^{(1)}(\text{space}) = (4\pi/3)^{1/2} Y_0^{(1)}(\hat{r}_{\text{space}}) = (4\pi/3)^{1/2} \sum_\lambda D_{0\lambda}^{(1)*}(\hat{R}) Y_\lambda^{(1)}(\hat{r}_{\text{mol}}). \quad \text{(A22)}$$

In Eq. (A22) we have assumed that r is of unit length and is only proportional to $Y_0^{(1)}$. Bray and Hochstrasser used a different normalization: they equated r with $Y_0^{(1)}$. Consequently, we pick up a factor of $(4\pi/3)^2$ when comparing our results with those of BH [see Eqs. (26)–(28)]. Substituting Eqs. (A21) and (A22) into the matrix element of Eq. (A20) and using E.4.2.7 and E.4.6.2 (note: these two equations agree with those in Appendix V of BS) we get

$$\begin{aligned}(2|r_0^{(1)}|1) &= (\gamma_2 v_2 J_2 M_2 \Lambda_2 | r_0^{(1)} | \gamma_1 v_1 J_1 M_1 \Lambda_1) \\ &= \sum_\lambda (-1)^{-\lambda} (4\pi/3)^{1/2} [\gamma_2 v_2 J_2 M_2 \Lambda_2 | D_{0-\lambda}^{(1)}(\hat{R}) Y_\lambda^{(1)}(\hat{r}_{\text{mol}}) | \gamma_1 v_1 J_1 M_1 \Lambda_1] \\ &= \sum_\lambda (-1)^{-\lambda} (4\pi/3)^{1/2} [(2J_2+1)(2J_1+1)]^{1/2} (-1)^{(M_1-\Lambda_1)} \\ &\quad \times \begin{pmatrix} J_2 & 1 & J_1 \\ M_2 & 0 & -M_1 \end{pmatrix} \begin{pmatrix} J_2 & 1 & J_1 \\ \Lambda_2 & -\lambda & -\Lambda_1 \end{pmatrix} r_{21}^{(\Lambda_2-\Lambda_1)}, \end{aligned} \quad \text{(A23)}$$

where

$$r_{21}^{(\Lambda_2-\Lambda_1)} = \int dR\, \chi_{v_2}(R) \langle \Psi_{\gamma_2}^{(e)}(\{\mathbf{r}_i'\};R) | Y_\lambda^{(1)}(\hat{r}_{\text{mol}}) | \Psi_{\gamma_1}^{(e)}(\{\mathbf{r}_i'\};R) \rangle \chi_{v_1}(R). \quad \text{(A24a)}$$

To get the total radial part of the transition dipole moment, we sum all the radial terms divided by their respective energy denominators:

$$R_{ei}^{(\Lambda_e-\Lambda_i)} = \sum_{\gamma_e} r_{ei}^{(\Lambda_e-\Lambda_i)}/D_{ei}; \quad R_{ei}'^{(\Lambda_e'-\Lambda_i)} = \sum_{\gamma_e'} r_{ei}'^{(\Lambda_e'-\Lambda_i)}/D_{ei}', \quad \text{(A24b)}$$

$$R_{fe}^{(\Lambda_f-\Lambda_e)} = r_{fe}^{(\Lambda_f-\Lambda_e)}; \quad R_{fe}^{(\Lambda_f-\Lambda_e)} = r_{fe}^{(\Lambda_f-\Lambda_e)}. \quad \text{(A24c)}$$

From the bottom row of the 3-j symbols in Eq. (A23) we get two identities: $M_1 = M_2$ and $\lambda = \Lambda_2 - \Lambda_1$. Substituting these into Eq. (A23) and negating the signs of the bottoms row of both 3-j symbols while performing an even permutation of the columns of the second 3-j symbol (E.3.7.4):

$$(v_2 J_2 M \Lambda_2 | r_0^{(1)} | v_1 J_1 M \Lambda_1) = (-1)^{(M-\Lambda_2)} R_{21}^{(\Lambda_2-\Lambda_1)} [(4\pi/3)(2J_2+1)(2J_1+1)]^{1/2} \times \begin{pmatrix} J_2 & 1 & J_1 \\ -M & 0 & M \end{pmatrix} \begin{pmatrix} J_1 & J_2 & 1 \\ \Lambda_1 & -\Lambda_2 & \Lambda_2-\Lambda_1 \end{pmatrix} R_{21}^{(\Lambda_2-\Lambda_1)}. \quad \text{(A25)}$$

Substituting Eq. (A25) into Eq. (A20) we arrive at a compact expression for the reduced matrix element of the dipole moment operator:

$$(J_2\Lambda_2 \| r^{(1)} \| J_1\Lambda_1) = (4\pi/3)^{1/2} R_{21}^{(\Lambda_2-\Lambda_1)} (2J_2+1)^{1/2} (2J_1+1)^{1/2} (-1)^{(J_2-\Lambda_2)} \begin{pmatrix} J_1 & J_2 & 1 \\ \Lambda_1 & -\Lambda_2 & \Lambda_2-\Lambda_1 \end{pmatrix}. \quad \text{(A26)}$$

4. The geometric term

The geometric term will first be calculated in the detector reference frame and later be calculated in the lab frame. These frames of reference were defined in Sec. II H. In what follows, all vectors are expressed in terms of their coordinates in the detector frame. We have assumed that the two-photon absorption is achieved using single-color linearly polarized light propagating along the y_d axis of the detector reference frame.[40] First, this implies that the photons are identical. Second, this forces ϕ_d to be zero so that the spherical tensors describing the photons are real:

Downloaded 02 Jun 2011 to 171.66.83.218. Redistribution subject to AIP license or copyright; see http://jcp.aip.org/about/rights_and_permissions

$$\hat{\mathbf{e}}_a = \hat{\mathbf{e}}_a^* = \hat{\mathbf{e}}_d = \hat{\mathbf{e}}_d^*. \tag{A27}$$

Hence, we should be able to express $\epsilon_q^{(k)}(k_d,k_a;\Omega)$ as proportional to a single spherical harmonic multiplied by some coupling factors. Toward this end, we write out the terms from the three cross products in the equation for $\hat{\epsilon}$ in terms of the individual spherical harmonics describing the electric field vectors of the photons. We need to develop an expression for the cross product of two tensors in which the coupling term is a 3-j symbol. We start with E.5.1.5:

$$[A^{(k_1)}\times B^{(k_2)}]_q^{(k)} = \sum_m (k_1 m, k_2 q-m | kq) A_m^{(k_2)} B_{q-m}^{(k_2)}. \tag{A28}$$

Using E.3.7.3 we can convert the Clebsch–Gordan coefficient into a 3-j symbol:

$$[A^{(k_1)}\times B^{(k_2)}]_q^{(k)} = \sum_m (-1)^{(k_2-k_1-q)}(2k+1)^{1/2} \times \begin{pmatrix} k_1 & k_2 & k \\ m & q-m & -q \end{pmatrix} A_m^{(k_1)} B_{q-m}^{(k_2)}. \tag{A29}$$

We use Eq. (A29) to break up the middle cross product in Eq. (A7). We also make use of Eq. (A27) to force the photons to be equivalent and linearly polarized. Note for the remainder of this section, we will drop the arguments of the ϵ function and will omit the subscripts on e_a and e_d since they are equivalent:

$$\epsilon(\text{det}) = \sum_m (-1)^{(k_a-k_d-q)}(2k+1)^{1/2} \times \begin{pmatrix} k_d & k_a & k \\ m & q-m & -q \end{pmatrix} \times [e^{(1)}\times e^{(1)}]_m^{(k_d)} [e^{(1)}\times e^{(1)}]_{q-m}^{(k_a)}. \tag{A30}$$

We can equate the electric field vector of the photons with the spherical harmonic of θ and ϕ_d where the former is the angle of the polarization vector with respect to the z_d axis and the latter describes the propagation direction of the laser beam. Since the laser is propagating along the y_d axis, $\phi_d = 0$ and

$$e_q^{(1)} = (4\pi/3)^{1/2} Y_q^{(1)}(\theta,\phi_d=0) = (4\pi/3)^{1/2} Y_q^{(1)*}(\theta,\phi_d=0). \tag{A31}$$

In Eq. (A31) we have assumed that e is of unit length and is only proportional to $Y_0^{(1)}$. We employ Eqs. (A29) and (A31) to evaluate the two cross products in Eq. (A30). Instead of explicitly finding the indicated ranks and components we will find general ones and later substitute for the ones required in Eq. (A30):

$$[Y^{(1)}(\theta,0)\times Y^{(1)}(\theta,0)]_{q_3}^{(k_3)} = \sum_{m_3} (-1)^{-q_3}(2k_3+1)^{1/2} \times \begin{pmatrix} 1 & 1 & k_3 \\ m_3 & q_3-m_3 & -q_3 \end{pmatrix} Y_{m_3}^{(1)}(\theta,0) Y_{q_3-m_3}^{(1)}(\theta,0). \tag{A32}$$

We can express the product of two spherical harmonics of the same angles as a series of single spherical harmonics of the same angles since we assume that our spherical harmonics are real (E.4.6.5):

$$Y_{m_3}^{(1)}(\theta,0) Y_{q_3-m_3}^{(1)}(\theta,0) = \sum_{k_4,m_4} \{9(2k_4+1)/4\pi\}^{1/2} \begin{pmatrix} 1 & 1 & k_4 \\ m_3 & q_3-m_3 & m_4 \end{pmatrix} \begin{pmatrix} 1 & 1 & k_4 \\ 0 & 0 & 0 \end{pmatrix} Y_{m_4}^{(k_4)}(\theta,0). \tag{A33}$$

Substituting Eq. (A33) into Eq. (A32), we get

$$[Y^{(1)}(\theta,0)\times Y^{(1)}(\theta,0)]_{q_3}^{(k_3)} = \sum_{k_4,m_4} (-1)^{-q_3}(9/4\pi)^{1/2} \begin{pmatrix} 1 & 1 & k_4 \\ 0 & 0 & 0 \end{pmatrix} Y_{m_4}^{(k_4)}(\theta,0) \times \sum_{m_3} (2k_3+1)^{1/2}(2k_4+1)^{1/2} \begin{pmatrix} 1 & 1 & k_3 \\ m_3 & q_3-m_3 & -q_3 \end{pmatrix} \begin{pmatrix} 1 & 1 & k_4 \\ m_3 & q_3-m_3 & m_4 \end{pmatrix}. \tag{A34}$$

Hence we can use E.3.7.8 to simplify part of the above equation to read

$$\sum_{m_3} (2k_3+1)^{1/2}(2k_4+1)^{1/2} \begin{pmatrix} 1 & 1 & k_3 \\ m_3 & q_3-m_3 & -q_3 \end{pmatrix} \begin{pmatrix} 1 & 1 & k_4 \\ m_3 & q_3-m_3 & m_4 \end{pmatrix} = \delta_{k_3,k_4}\delta_{-q_3,m_4}\delta(1,1,k_3), \tag{A35}$$

where $\delta(1,1,k_3)$ implies that the three vectors obey the triangle condition.

Substituting Eq. (A35) into Eq. (A24) and replacing k_4 by k_3 and m_4 by $-q_3$ as required by the Dirac delta functions in Eq. (A35), we arrive at an equation for the cross product of two real spherical harmonics:

$$[Y^{(1)}(\theta,0)\times Y^{(1)}(\theta,0)]_{q_3}^{(k_3)} = (-1)^{-q_3}(9/4\pi)^{1/2} \begin{pmatrix} 1 & 1 & k_3 \\ 0 & 0 & 0 \end{pmatrix} Y_{-q_3}^{(k_3)}(\theta,0). \tag{A36}$$

Finally, we can simplify the tensor products in the equation for ϵ. Substituting Eq. (A31) four times and Eq. (A36) twice into Eq. (A30) we find

Downloaded 02 Jun 2011 to 171.66.83.218. Redistribution subject to AIP license or copyright; see http://jcp.aip.org/about/rights_and_permissions

$$\epsilon(\det) = (4\pi/3)^2 \sum_m (-1)^{(k_a - k_d - q)}(-1)^{m-q-m}(2k+1)^{1/2}(9/4\pi)$$

$$\times \begin{pmatrix} k_d & k_a & k \\ m & q-m & -q \end{pmatrix} \begin{pmatrix} 1 & 1 & k_d \\ 0 & 0 & 0 \end{pmatrix} \begin{pmatrix} 1 & 1 & k_a \\ 0 & 0 & 0 \end{pmatrix} Y^{(k_d)}_{-m}(\theta,0)\, Y^{(k_a)}_{m-q}(\theta,0). \tag{A37}$$

We can eliminate the phase factor by permuting the first two columns of the second and third 3-j symbols (E.3.7.5). Next we expand the product of the two real spherical harmonics into its tensor components (E.4.6.5) and negate the bottom rows of both 3-j symbols:

$$Y^{(k_d)}_{-m}(\theta,0)\, Y^{(k_a)}_{m-q}(\theta,0) = \sum_{k_6,m_6} [(2k_6+1)(2k_d+1)(2k_a+1)/4\pi]^{1/2}$$

$$\times \begin{pmatrix} k_d & k_a & k_6 \\ m & q-m & -m_6 \end{pmatrix} \begin{pmatrix} k_d & k_a & k_6 \\ 0 & 0 & 0 \end{pmatrix} Y^{(k_6)}_{m_6}(\theta,0). \tag{A38}$$

Substituting Eq. (A38) into Eq. (A37),

$$\epsilon(\det) = (4\pi/3)^2 \sum_{k_6,m_6} (9/4\pi)[(2k_d+1)(2k_a+1)/4\pi]^{1/2} Y^{(k_6)}_{m_6}(\theta,0) \begin{pmatrix} k_d & k_a & k_6 \\ 0 & 0 & 0 \end{pmatrix} \begin{pmatrix} 1 & 1 & k_d \\ 0 & 0 & 0 \end{pmatrix} \begin{pmatrix} 1 & 1 & k_a \\ 0 & 0 & 0 \end{pmatrix}$$

$$\times \sum_m (2k+1)^{1/2}(2k_6+1)^{1/2} \begin{pmatrix} k_d & k_a & k \\ m & q-m & -q \end{pmatrix} \begin{pmatrix} k_d & k_a & k_6 \\ m & q-m & -m_6 \end{pmatrix}. \tag{A39}$$

Once again we can remove two 3-j symbols using E.3.7.8 while gaining the useful identity:

$$\sum_m (2k+1)^{1/2}(2k_6+1)^{1/2} \begin{pmatrix} k_d & k_a & k \\ m & q-m & -q \end{pmatrix} \begin{pmatrix} k_d & k_a & k_6 \\ m & q-m & -m_6 \end{pmatrix} = \delta_{q,m_6}\delta_{k,k_6}\delta(k_d,k_a,k). \tag{A40}$$

Substituting Eq. (A40) into Eq. (A39) and replacing k_6 by k and m_6 by q we arrive at our final equation for the geometric term:

$$\epsilon(\det) = [4\pi(2k_d+1)(2k_a+1)]^{1/2} \begin{pmatrix} k_d & k_a & k \\ 0 & 0 & 0 \end{pmatrix} \begin{pmatrix} 1 & 1 & k_d \\ 0 & 0 & 0 \end{pmatrix} \begin{pmatrix} 1 & 1 & k_a \\ 0 & 0 & 0 \end{pmatrix} Y^{(k)}_q(\theta,0). \tag{A41}$$

Equation (A41) allows us to calculate the geometric term for all the alignment moments, but it does not remove the linear dependency between the different components of moments of the same rank. This is a result of the spherical harmonics being linearly independent over all space but linearly dependent when $\phi = 0$. To remove the linear dependency between the moments we must rotate the laser beam propagation direction with respect to the quantization axis of the molecules. Since Eq. (A41) already calculates ϵ in the detector frame, we only need to employ the rotation matrix coefficients to calculate ϵ in the lab frame. As explained in the previous section we have adopted the conventions of BrHd for transforming between space-fixed and molecule-fixed frames which implies that our rotation matrix coefficients are defined by the formalism of Brink and Satchler (BS). From Eq. (4.8) of BS,

$$\epsilon^{(k)}_q(k_d,k_a;\theta,0)(\text{lab}) = \sum_{q'} D^{(k)*}_{q,q'}(\phi_u,\theta_u,\chi_u)\epsilon^{(k)}_{q'}(k_d,k_a;\theta,0)(\det), \tag{A42}$$

where ϕ_u,θ_u,χ_u are the Euler angles which rotate the lab frame into the detector frame. The Euler angles must be chosen so that θ remains unchanged and $\phi = 0$ in both frames. Using this equation one can evaluate the geometric term for any detector geometry involving linearly polarized light. We can greatly simplify Eq. (A42) by assuming the detector always lies in the x–y plane of the lab frame. This allows us to set $\phi_u = 0$, $\theta_u = 0$, and $\chi_u = \chi$, where χ is defined as the angle between the laser propagation direction and the y axis of the lab frame. Under these assumptions [see Eqs. (2.15)–(2.19) of BS]:

$$D^{(k)*}_{q,q'}(\phi_u,\theta_u,\chi_u) = D^{(k)*}_{q,q'}(0,0,\chi) = d^k_{q',q}(0)e^{iq'\chi} = \delta_{q,q'}e^{iq'\chi}. \tag{A43}$$

Substituting Eq. (A43) into Eq. (A42), we get

$$\epsilon^{(k)}_q(k_d,k_a;\theta,0,\chi)(\text{lab}) = e^{iq\chi}\epsilon^{(k)}_q(k_d,k_a;\theta,0,\chi)(\det). \tag{A44}$$

Substituting Eq. (A41) into Eq. (A44) we get a general expression for ϵ(lab) for the case where the detector lies anywhere in the x–y plane of the lab frame:

$$\epsilon^{(k)}_q(\text{lab}) = [4\pi(2k_d+1)(2k_a+1)]^{1/2} \times \begin{pmatrix} k_d & k_a & k \\ 0 & 0 & 0 \end{pmatrix} \begin{pmatrix} 1 & 1 & k_d \\ 0 & 0 & 0 \end{pmatrix} \times \begin{pmatrix} 1 & 1 & k_a \\ 0 & 0 & 0 \end{pmatrix} Y^{(k)}_q(\theta,0)e^{iq\chi}. \tag{A45}$$

It is important to note that Eq. (A45) still restricts us to even ranks; linearly polarized light can never detect the orientations of molecules in any frame of reference. Second, for even q, the real part of $\epsilon^{(k)}_q$ and $\epsilon^{(k)}_{-q}$ are equal while their imaginary parts are of opposite sign; for odd q, the opposite is true. This treatment is restricted to two photons of the same linear

Downloaded 02 Jun 2011 to 171.66.83.218. Redistribution subject to AIP license or copyright; see http://jcp.aip.org/about/rights_and_permissions

polarization, i.e., it does not apply to unpolarized or incoherent excitation.

5. The hyperfine depolarization factor

So far we have treated the two-photon absorption as being a time independent process; this is not sufficient if **J** is coupled to either the nuclear spin **I** or the electron spin **S**. In either case, at time $t=0$, the instant the ground state distribution has been prepared, $\mathbf{J}_i$ will be pointing a specific direction indicative of the initial ground state distribution. But due to its coupling with either **I** or $\mathbf{S}_i$, at time $t>0$, $\mathbf{J}_i$ will be pointing at a different direction. This loss of alignment has been calculated in the $t\rightarrow\infty$ limit by FM and GZ. From Eq. (37) of Greene and Zare[22] we derived Eq. (10) and Eq. (11) by assuming $\omega_{F',F}\gg\tau^{-1}$, i.e., $\mathbf{J}_i$ precesses many times around $\mathbf{F}_i$ before the molecule is detected and by summing Eq. (37) of Greene and Zare[22] over I and S and multiplying by the degeneracies, $(2I+1)$ and $(2S+1)$. Thus for $k=0$ the depolarization factor equals the total electronic and nuclear spin degeneracy for all the states coupled to a particular J_i.

6. Matrix elements of the spherical tensor angular momentum operator

The intensity expression given by Eq. (A5) includes two sets of complex spherical tensor operators, $\epsilon_q^{(k)}$ and $J_q^{(k)}$; this is most inconvenient. When numerically calculating the line strengths, it is much easier to work with real quantities. Using the formalism of Hertel and Stoll[41] we can convert to an intensity equation containing only real quantities. First we must segregate all the terms which do not dependent on the sign of q since they are real quantities; this collection of real functions we designate as F^{real}:

$$I=\sum_{k_d,k_a,k}F^{\text{real}}\sum_{q=-k}^{k}\langle(J_iM_i\Lambda_i|J_{-q}^{(k)}|J_iM_i\Lambda_i)\rangle\epsilon_q^{(k)}$$
$$=\sum_{k_d,k_a,k}F^{\text{real}}\sum_{q=0}^{k}[\langle(J_iM_i\Lambda_i|J_{-q}^{(k)}|J_iM_i\Lambda_i)\rangle\epsilon_{+q}^{(k)}$$
$$+\langle(J_iM_i\Lambda_i|J_{+q}^{(k)}|J_iM_i\Lambda_i)\rangle\epsilon_{-q}^{(k)}](1+\delta_{0,q})^{-1}, \tag{A46}$$

where

$$\epsilon_q^{(k)}=\epsilon_q^{(k)}(k_d,k_a,k;\Omega_{\text{lab}}), \tag{A47}$$

$$F^{\text{real}}=(-1)^{k-q}CZ/(J_i\|J^{(k)}\|J_i), \tag{A48}$$

and C and Z are defined in Eqs. (A1) and (A18), respectively.

Next, we write out the definition of the "real tensor operators" as given by Hertel and Stoll and then invert the definitions:

$$T_{q\pm}^{\{k\}}=(1/2)^{-1/2}(i)^{(\pm1-1)/2}$$
$$\times[(-1)^qT_{+q}^{(k)}\pm T_{-q}^{(k)}]\quad\text{for } 0<q\leqslant k, \tag{A49a}$$

$$T_{0+}^{\{k\}}=T_{+0}^{(k)};\quad T_{0-}^{\{k\}}=0, \tag{A49b}$$

$$T_{\pm q}^{(k)}=(1/2)^{-1/2}(-1)^{q(\mp1-1)/2}$$
$$\times[T_{q+}^{\{k\}}\pm iT_{q-}^{\{k\}}]\quad\text{for } 0<q\leqslant k. \tag{A49c}$$

The braces around k indicate that $T_{q\pm}^{\{k\}}$ is a real tensor operator as opposed to a spherical tensor operator, $T_{\pm q}^{(k)}$.

We can change our intensity equation from a summation over the complex tensor operators to one over real operators by substituting Eq. (A49c) into Eq. (A46) four times:

$$I=\sum_{k_d,k_a,k}F^{\text{real}}\sum_{q=0}^{k}(-1)^{-q}$$
$$\times[\langle(J_iM_i\Lambda_i|J_{q+}^{\{k\}}|J_iM_i\Lambda_i)\rangle\epsilon_{q+}^{\{k\}}$$
$$+\langle(J_iM_i\Lambda_i|J_{q-}^{\{k\}}|J_iM_i\Lambda_i)\rangle\epsilon_{q-}^{\{k\}}]. \tag{A50}$$

We want to break up the intensity expression so that it is factored into a sum of terms each of which is a real moment of the ground state distribution multiplied by a real tensor moment of the line strength. In Eq. (A50) the moments of the ground state distribution are real, but they do not have definite limits. First, we normalize the ground state rank k moments to force them to agree with the FM conventions by multiplying them by $c(k)[J_i(J_i+1)]^{-k/2}$; $c(k)$ has already been defined in Eqs. (7a)–(7c). These GZ normalized components have their rank denoted by $\{k\}$ where the braces indicate that $A_q^{\{k\}}$ is a real spherical tensor operator. Second, we create a quantity, $P_q^{\{k\}}$, which contains all the factors in the intensity equation which depends on k and q; here the braces on k indicate that $P_q^{\{k\}}$ contains sums of the real tensor operator, $\epsilon_{q\pm}^{\{k\}}$. Third, the normalization constant C is factored into the population of the ground state $n(J_i)$, and a factor $C(\text{det})$, which represents the dependence on the laser intensity, the sensitivity of the detector, etc.:

$$A_{q\pm}^{\{k\}}(J_i)=c(k)\langle(J_iM_i\Lambda_i|J_{q\pm}^{\{k\}}|J_iM_i\Lambda_i)\rangle/[(J_iM_i\Lambda_i|\mathbf{J}^2|J_iM_i\Lambda_i)]^{k/2}, \tag{A51}$$

$$b^k(J_i)=c(k)^{-1}\{[(J_iM_i\Lambda_i|\mathbf{J}^2|J_iM_i\Lambda_i)]^{k/2}\}/(J_i||J^{(k)}||J_i), \tag{A52}$$

$$P_{q\pm}^{\{k\}}(J_i,\Lambda_i,J_f,\Lambda_f;\Omega)=b^k(J_i)g^k(J_i)\sum_{k_d,k_a}(-1)^k\epsilon_{q\pm}^{\{k\}}(k_d,k_a;\Omega)\sum_{J_e,\Lambda_e,J_e',\Lambda_e'}$$
$$\times S(J_i,\Lambda_i,J_e,\Lambda_e,J_e',\Lambda_e',J_f,\Lambda_f)h(k_d,k_a,k,J_i,J_e,J_e',J_f), \tag{A53}$$

$$h(k_d,k_a,k,J_i,J_e,J_e',J_f)=(-1)^{(J_f+J_e'-k_d+1)}[(2k_d+1)(2k_a+1)(2k+1)]^{1/2}\begin{Bmatrix}J_e' & J_e & k_d\\ 1 & 1 & J_f\end{Bmatrix}\begin{Bmatrix}J_e' & 1 & J_i\\ J_e & 1 & J_i\\ k_d & k_a & k\end{Bmatrix}, \tag{A54}$$

$$C=C(\text{det})n(J_i). \tag{A55}$$

Note, we have added the hyperfine depolarization factor into this equation. If there is spin depolarization, $g^k(N_i)$ should

Downloaded 02 Jun 2011 to 171.66.83.218. Redistribution subject to AIP license or copyright; see http://jcp.aip.org/about/rights_and_permissions

replace $g^k(J_i)$ for case (b) coupling. The $b^k(J_i)$ are tabulated in Table VII and are identical to those of GZ but differ from those of CMH by a factor of $(2J_i+1)^{-1/2}$; this results from a difference in the conventions employed in defining reduced matrix elements. We can now substitute Eqs. (A51)–(A55) into the equation for the intensity, Eq. (A50), after identifying Z with Eq. (A18),

$$I = C(\det) \sum_{k,q} [P_{q+}^{\{k\}}(J_i,\Lambda_i,J_f,\Lambda_f;\Omega) A_{q+}^{\{k\}}(J_i) + P_{q-}^{\{k\}}(J_i,\Lambda_i,J_f,\Lambda_f;\Omega) A_{q-}^{\{k\}}(J_i)] n(J_i). \tag{A56}$$

The above equation is completely general.

7. Orthogonal excitation–detection geometry

For the special case of excitation with linearly polarized light propagating along the y axis of the lab frame, Eq. (A56) can be greatly simplified. For this case, we can always assume that the geometric term ϵ, and the moments of the ground state are purely real. Equations (A49a) and (A49b) can be rewritten:

$$T_{q+}^{\{k\}} = (-1)^q [D(q)]^{1/2} \mathrm{Re}(T_{+q}^{(k)}), \tag{A57a}$$

$$T_{q-}^{\{k\}} = (-1)^q [D(q)]^{1/2} \mathrm{Im}(T_{+q}^{(k)}), \tag{A57b}$$

$$D(q=0) = 1, \tag{A57c}$$

$$D(q\neq 0) = 2. \tag{A57d}$$

For this case that the lab and detector frames coincide, Eq. (A41) defines ϵ in the lab frame as being real; hence $\epsilon_{q-}^{\{k\}} = 0$ and we can drop a term in Eq. (A56). We pick up $(-1)^q$ factors from both $A_q^{\{k\}}$ and $\epsilon_q^{\{k\}}$ and, hence, these phase factors cancel. Using Eq. (A57) to simplify the remaining term,

$$I = C(\det) \sum_{k,q} P_q^k(J_i,\Lambda_i,J_f,\Lambda_f;\Omega_{\mathrm{lab}}) A_q^{(k)}(J_i) n(J_i), \tag{A58}$$

where

$$P_q^k(J_i,\Lambda_i,J_f,\Lambda_f;\Omega_{\mathrm{lab}}) = D(q) b^k(J_i) g^k(J_i) \sum_{k_d,k_a} (-1)^k \epsilon(k_d,k_a,k,q;\Omega_{\mathrm{lab}}) \times \sum_{J_e,\Lambda_e,J_e',\Lambda_e'} S(J_i,\Lambda_i,J_e,\Lambda_e,J_e',\Lambda_e',J_f,\Lambda_f) \times h(k_d,k_a,k,J_i,J_e,J_e',J_f) \tag{A59}$$

and

$$A_q^{(k)}(J_i) = c(k) \mathrm{Re}\langle (J_i M_i \Lambda_i | J_{+q}^{(k)} | J_i M_i \Lambda_i) \rangle / [(J_i M_i \Lambda_i | \mathbf{J}^2 | J_i M_i \Lambda_i)]^{k/2}, \tag{A60}$$

$$\epsilon(k_d,k_a,k,q;\Omega_{\mathrm{lab}}) = \epsilon(k_d,k_a,k,q;\Omega_{\mathrm{det}}) = \epsilon_q^{(k)}(k_d,k_a;\Omega). \tag{A61}$$

We have omitted the signs on q and the brackets around k on the P_q^k to distinguish them from the $P_{q\pm}^{\{k\}}$ defined in Eq. (A53). The signs on q were omitted and parentheses were substituted for braces around k on the $A_q^{(k)}$ to distinguish them from the real tensor operators, $A_{q\pm}^{\{k\}}$ defined in Eq. (A51). P_q^k and $A_q^{(k)}$ are neither spherical tensor operators nor real tensor operators; they are just parameters in our equation for the intensity.

We have now derived the intensity equation for single-color two-photon excitation under three conditions: (1) general detection geometry; (2) detection in the $x-y$ plane of the lab frame, and (3) detection along the y axis of the lab frame. All the relevant equations along with their restrictions are given in Tables I–IV.

[1] D. A. Case, G. M. McClelland, and D. R. Herschbach, Mol. Phys. **35**, 541 (1978).
[2] C. H. Greene and R. N. Zare, J. Chem. Phys. **78**, 6741 (1983).
[3] U. Fano and J. H. Macek, Rev. Mod. Phys. **45**, 553 (1973).
[4] M. D. Rowe and A. J. McCaffery, Chem. Phys. **43**, 35 (1979); A. J. Bain, A. J. McCaffery, M. J. Proctor, and B. J. Whitaker, Chem. Phys. Lett. **110**, 663 (1984); A. J. Bain and A. J. McCaffery, *ibid*, **105**, 477 (1984); **108**, 275 (1984); J. Chem. Phys. **80**, 5883 (1984); **83**, 2627, 2632, 2641 (1985).
[5] D. C. Jacobs and R. N. Zare, J. Chem. Phys. **85**, 5457 (1986).
[6] R. G. Bray and R. M. Hochstrasser, Mol. Phys. **31**, 1199 (1976).
[7] W. M. McClain and R. A. Harris, in *Excited States*, edited by E. C. Lim (Academic, New York, 1977), Vol. 3, pp. 1–56.
[8] J. B. Halpern, H. Zacharias, and R. Wallenstein, J. Mol. Spectrosc. **79**, 1 (1980).
[9] K. Chen and E. S. Yeung, J. Chem. Phys. **70**, 1312 (1979).
[10] M. Dubs, U. Brühlmann, and J. R. Huber, J. Chem. Phys. **84**, 3106 (1986).
[11] W. M. McClain, J. Chem. Phys. **55**, 2789 (1971).
[12] M. A. C. Nascimento, Chem. Phys. **74**, 51 (1983).
[13] P. R. Monson and W. M. McClain, J. Chem. Phys. **53**, 29 (1970).
[14] J. Michl and E. W. Thulstrup, J. Chem. Phys. **72**, 3999 (1980); E. W. Thulstrup and J. Michl, Int. J. Quantum Chem. Symp. **17**, 471 (1983).
[15] E. E. Marinero, C. T. Rettner, and R. N. Zare, Phys. Rev. Lett. **48**, 1323 (1982).
[16] S. T. Pratt, P. M. Dehmer, and J. L. Dehmer, J. Chem. Phys. **80**, 1706 (1984); **81**, 3444 (1984); K. L. Carleton, K. H. Welge, and S. R. Leone, Chem. Phys. Lett. **115**, 492 (1985).
[17] R. W. Jones, N. Sivakumar, B. H. Rockney, P. L. Houston, and E. R. Grant, Chem. Phys. Lett. **91**, 271 (1982); G. W. Loge, J. J. Tiee, and F. B. Wampler, J. Chem. Phys. **79**, 196 (1983).
[18] D. Zakheim and P. Johnson, J. Chem. Phys. **68**, 3644 (1978).
[19] A. Sur, C. V. Ramana, and S. D. Colson, J. Chem. Phys. **83**, 904 (1985).
[20] S. Arepalli, N. Presser, D. Robie, and R. J. Gordon, Chem. Phys. Lett. **118**, 88 (1985).
[21] L. C. Biedenharn, Ann. Phys. **4**, 104 (1958).
[22] C. H. Greene and R. N. Zare, Annu. Rev. Phys. Chem. **33**, 119 (1982).
[23] J. A. Guest, M. A. O'Halloran, and R. N. Zare, Chem. Phys. Lett. **103**, 261 (1984).
[24] J. Mathews, *Tensor Spherical Harmonics* (Graphic Arts, California Institute of Technology, Pasadena, CA, 1981).
[25] L. Pauling and E. B. Wilson, *Introduction to Quantum Mechanics* (McGraw-Hill, New York, 1935).
[26] M. E. Rose, *Elementary Theory of Angular Momentum* (Wiley, New York, 1957).
[27] U. Fano and G. Racah, *Irreducible Tensorial Sets* (Academic, New York, 1959).
[28] M. Rotenberg, R. Bivins, N. Metropolis, and J. K. Wooten, Jr., *The 3-j and 6-j Symbols* (MIT, Cambridge, Massachusetts, 1959).
[29] A. R. Edmonds, *Angular Momentum in Quantum Mechanics*, 2nd ed. (Princeton University, Princeton, 1974).
[30] D. M. Brink and G. R. Satchler, *Angular Momentum*, 2nd ed. (Clarendon, Oxford, 1968).
[31] R. N. Zare, A. L. Schmeltekopf, W. J. Harrop, and D. L. Albritton, J. Mol. Spectrosc. **46**, 37 (1973).

Downloaded 02 Jun 2011 to 171.66.83.218. Redistribution subject to AIP license or copyright; see http://jcp.aip.org/about/rights_and_permissions

[32]E. E. Marinero, R. Vasudev, and R. N. Zare, J. Chem. Phys. **78**, 692 (1983).
[33]This is particularly convenient for N_2 where there are only two branches which are unblended, the *O* and *P* branches.
[34]A. C. Kummel, G. O. Sitz, and R. N. Zare (in preparation).
[35]G. O. Sitz, A. C. Kummel, and R. N. Zare (in preparation).
[36]S. N. Dixit and V. McKoy, J. Chem. Phys. **82**, 3546 (1985).
[37]J. M. Brown and B. J. Howard, Mol. Phys. **31**, 1517 (1976).
[38]M. Bouten, Physica **42**, 572 (1969).
[39]M. Larsson, Phys. Scr. **23**, 835 (1981).
[40]U. Fano, J. Opt. Soc. Am. **39**, 859 (1949).
[41]I. V. Hertel and W. Stoll, Adv. At. Mol. Phys. **13**, 113 (1978).

Downloaded 02 Jun 2011 to 171.66.83.218. Redistribution subject to AIP license or copyright; see http://jcp.aip.org/about/rights_and_permissions